NUREG/CR-1377
SAND80-0644
GF

RISK METHODOLOGY FOR GEOLOGIC DISPOSAL OF RADIOACTIVE WASTE: TRANSPORT MODEL SENSITIVITY ANALYSIS

James E. Campbell and Ronald L. Iman
Sandia National Laboratories
Albuquerque, New Mexico 87185

and

Mark Reeves
INTERA Environmental Consultants
Houston, Texas 77079

Date Published: June 1980

Sandia National Laboratories
Albuquerque, New Mexico 87185
operated by
Sandia Corporation
for the
U.S. Department of Energy

Prepared for
Office of Nuclear Regulatory Research
Probabilistic Analysis Staff
U.S. Nuclear Regulatory Commission
Washington, DC 20555
Under Memorandum of Understanding DOE 40-550-75
NRC FIN No. A-1192

ABSTRACT

In this report, a sensitivity analysis methodology is demonstrated for geosphere transport. The sensitivity analysis uses two transport simulators. One simulator is the general, multidimensional numerical model SWIFT. The other is the simplified network flow model NWFT, which contains a one-dimensional radionuclide transport simulator. Statistical techniques used in the sensitivity analysis include Latin hypercube sampling and stepwise regression on ranks. The demonstration problems are based on a reference site geology and hydrology which, although hypothetical, contain properties of real sites. Three different waste release scenarios are examined.

CONTENTS

I. INTRODUCTION

Risk analysis is a vital part of any safety assessment of a proposed nuclear waste depository. Risk analysis results are expressed in terms of radiation-induced health effects and are calculated using mathematical models which describe the following processes: (1) radionuclide migration in groundwater from the depository to a discharge point in the surface environment, (2) radionuclide migration and accumulation in the surface environment, (3) human uptake, and (4) radiation dosimetry and health effects. There are large uncertainties associated with many of the input variables to these models so that ranges, rather than point values, are often specified. Consequently, the risk estimates themselves have large uncertainties. Therefore, point estimates of risk, without an indication of the possible distribution of results, are probably meaningless and may be misleading.

Given the importance of quantifying uncertainties in risk estimates, it is clearly important to identify those input variables which are major contributors to variation in model output. Not only does this facilitate the analysis of risk, but it also aids in establishing field-research priorities. Statistical techniques have beer developed to study the sensitivity of model output to model input. These statistical methods can be found in Iman, Helton and Campbell [1978]. The research reported here represents field-scale applications of these methods to a model for radionuclide migration in groundwater from a depository to a discharge point.

In Chapter II, the statistical techniques for sensitivity analysis given in Iman, Helton and Campbell [1978] are briefly reviewed. Chapter III describes the hypothetical waste repository site which provides the geologic setting for the analyses presented in this report.

In Chapter IV, a point is made which is quite important for future sensitivity and risk analyses, namely that simplified, analytical models can yield reliable results for sensitivity and risk analyses. Two transport models, named SWIFT and NWFT, are used. The former is the Sandia Waste Isolation Flow and Transport Model [Dillon, Lantz, and Pahwa, 1978]. It is a three-dimensional, finite-difference model which solves conservation equations for fluid flow, heat transport, (possibly nontrace) solute mass, and radionuclides in trace quantities. The latter model is the Network Flow and Transport Model [Campbell, et al., 1980] which solves a two-dimensional network at steady state to obtain the fluid flow and then analytically solves for the radionuclide transport along the radionuclide migration path through the network. Also in Chapter IV, a SWIFT sensitivity analysis is compared with a NWFT sensitivity analysis for the same U-tube breachment scenario to demonstrate the applicability of the computationally efficient, but simplified, NWFT model for sensitivity analysis.

Another point is made in Chapter V which is also important for future risk assessments. The point is that sensitivity analysis

may be performed on a few selected scenarios to single out variables to be considered in a risk analysis without the necessity for performing a sensitivity analysis on each individual scenario. This conclusion is supported by considering that, for a given depository breachment scenario, the radionuclide discharge to the environment is essentially controlled by three principal system characteristics; (1) the time at which circulating groundwater first contacts the radioactive waste, (2) the rate at which radionuclides enter solution (i.e., the source rate) and (3) the migration time from the depository to a discharge point to the environment. The time of first groundwater contact is not addressed in this report but, rather, is addressed in estimating scenario probabilities. Here it is assumed that depository breachment scenarios occur, and the sensitivity of total radionuclide discharge to depository, hydrologic and geochemical variables which control the radionuclide source rate and migration time is examined.

Results and conclusions of this study are summarized in Chapter VI. This study did not consider the effects of variables arising through models for surface environment pathways or human uptake and dosimetry. Our rationale here is threefold: First, the objective here is to demonstrate that the methodology of sensitivity analysis is applicable to the submodel which is most complex, namely the geosphere transport. Second, we contend that since the depository and the geologic media surrounding it provide the primary containment of the nuclear waste, the variables describing the media are consequently most important for consideration by a sensitivity

analysis. Third, since there is no back coupling, i.e., geosphere transport does not depend upon surface environment transport for example, sensitivity considerations may likewise be uncoupled. Sensitivity analysis results are on the Pathways to Man Model is reported by Helton and Iman [1980].

The work reported here is part of a program funded at Sandia National Laboratories by the Nuclear Regulatory Commission to develop a risk assessment methodology for the geologic disposal of radioactive wastes.

II. REVIEW OF SENSITIVITY ANALYSIS TECHNIQUES

Before proceeding with the sensitivity analyses of disruptive-event scenarios for the reference site it is appropriate to review both the sensitivity techniques to be used and the motivation for using them. These items are covered thoroughly in Iman, Helton, and Campbell [1978]. The objective here is to provide a brief review of the statistical techniques used.

There are two primary reasons for applying sensitivity methods. The first is to ascertain which variables have a statistically significant effect upon total discharge. The term "significant" is, in this report, taken to mean "significant at approximately the 5 percent level." In addition, it may be necessary to determine the relative importance of the various variables in source-rate and migration-time dominated regimes. The second primary reason is to determine the relationship between model output and distribution assumptions on model input. Not only may there be uncertainty in

the values of input variables but also there may be uncertainty in the distributions chosen for the input variables. It may be desirable to assess this effect [Iman, Helton, and Campbell, 1978].

2.1 Response-Surface Construction

The focal point of the sensitivity analysis used in this work is the construction of the response surface. Conceptually the idea of a response surface is based on a simple geometrical picture such as that shown in Figure 1 for a case involving only two independent variables. The dependent variable Y is given as a function of the two independent variables X_1 and X_2 over their respective ranges. (Selection of specific values of X_1 and X_2 is considered in the next subsection.) Surface S is the response surface. In general, the value of the dependent variable Y is known only at certain discrete points (i.e., for particular combinations of X_1 and X_2) as indicated by the crosses in Figure 1. In the physical problem addressed in this paper, the discrete points are known as a result of transport calculations with either the SWIFT code or the NWFT code.

Although simple in concept, response-surface construction involves several statistical procedures. There is, for example, preliminary variable assessment using partial correlation coefficients, stepwise regression for construction of the response surface, protection against overfit, use of t-tests to establish significance levels for the independent variables, and various tests to examine the effect of input variable distribution assumptions on the output variable distribution. Details of

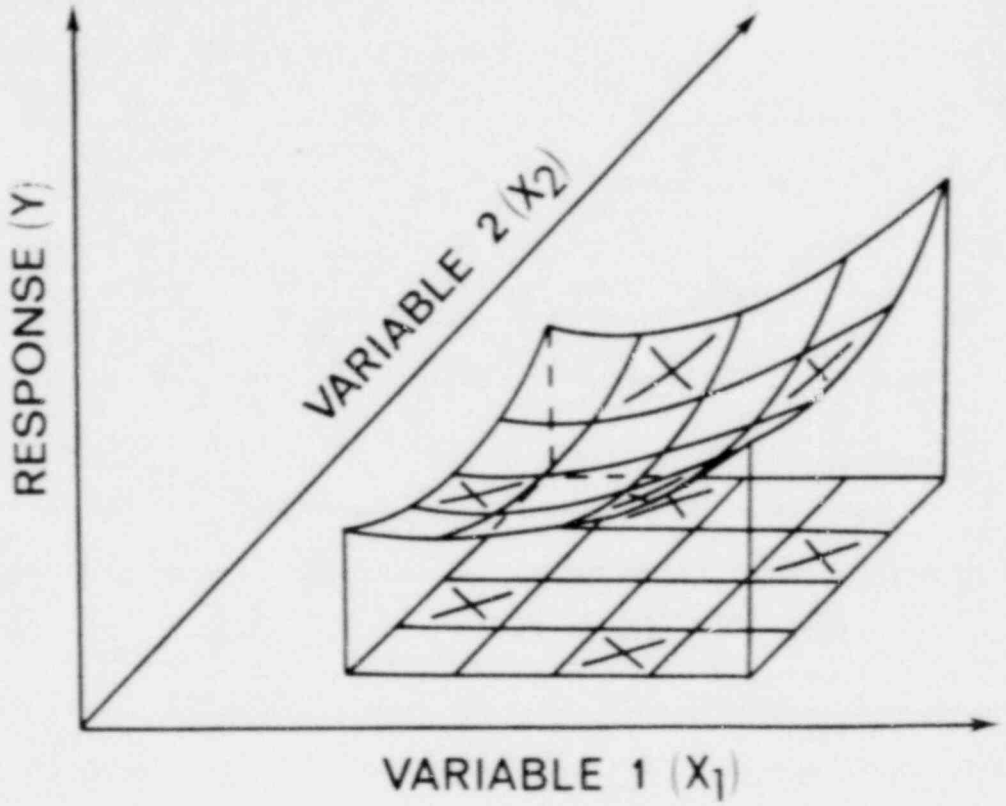

Figure 1. Conceptualization of a Response Surface for Two Independent Variables.

these procedures can be found in Iman, Helton and Campbell [1978] and in references cited therein.

The fitting of the response surface by stepwise regression is of central importance to the sensitivity analysis as this process selects the important independent variables as well as providing an ordering of the relative importance of the independent variables on the basis of standardized regression coefficients. Once the response surface has been constructed and validated, it may be used to assess the effect of the distribution assumptions made on each of the significant input variables.

2.2 Input Variable Selection

As may have been inferred from Figure 1, to perform sensitivity analysis on a model, it is necessary to obtain model output for various values of the input variables. Latin Hypercube Sampling (LHS) is used as a selection technique to obtain model input values. LHS minimizes, relative to other commonly used sampling schemes, the number of model calculations required for response surface construction when the output is a monotone function of the input [McKay, Conover and Beckman, 1979]. LHS produces a global selection of points which provide an unbiased estimate of cumulative distribution functions and mean values for the model output. A brief description of LHS is provided in the following discussion.

Consider the simple two variable case illustrated in Figure 1 and assume that 4 input vectors will be generated. First, the range of each variable is divided into 4 nonoverlapping intervals

based on equal width or equal probability as shown in the illustration below

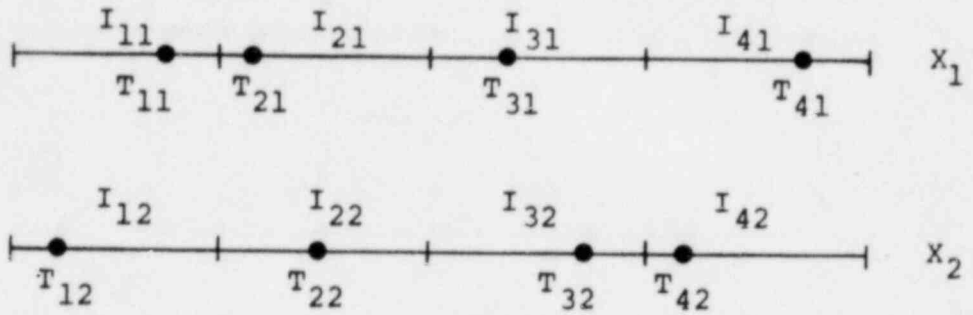

Values T_{ij} are randomly selected from intervals I_{ij} as shown above. Finally, 4 input vectors (T_{k1}, T_{m2}) k, m = 1, 2, 3, 4 are formed by randomly selecting, without replacement, from the 4 previously selected values of X_1 and X_2.

2.3 Rank Transformation

Another important technique which we wish to review is rank regression [Iman and Conover, 1979]. The motivation here stems from the nonlinearity which is frequently present in the dependence $Y = f(X_1, X_2, \ldots)$ of the basic response variable upon the independent variables. If, however, the dependence is monotone, as it frequently is for transport calculations, then it may be linearized with the rank transformation. The concept of a rank transform is simple in that each variable (independent and dependent) is replaced by its corresponding rank. For example, the smallest values of X_i is replaced by the rank 1, the next smallest by the rank 2, and so on. Thus the original discrete valued function is replaced by the rank-transformed function $R(Y) = f[R(X_1), R(X_2), \ldots]$. It is this transformed function which is estimated using

stepwise regression and which is used to establish the significance and relative importance of the independent variables.

III. THE REFERENCE SITE

The reference site is entirely hypothetical, yet its physiographic setting and geologic and hydrologic properties are real in the sense that they were chosen as equivalent to those in several regions in the United States. This site is located in a symmetrical upland valley, half of which is shown schematically in Figure 2. The crest of the ridge surrounding the valley is at an elevation of 6000 feet, and the crest is a surface- and groundwater divide so that the only water moving in the valley falls in the valley itself. The valley is drained by a major river, River L, which is at elevation 2500 feet. Stream valleys tributary to River L exist, such as River U, but they are normally dry. The valley receives 40 inches of rainfall per year, of which 16 inches are lost by evapotranspiration and the remaining 24 inches recharge the ground water system.

The geologic properties of the site are shown in cross section in Figure 3. The valley is underlain by crystalline bedrock which crops out only over a narrow width at the ridge crest surrounding the valley. This bedrock is assumed to be impermeable to groundwater flow. Above the bedrock is a sequence of sedimentary rock as shown in Figure 3. Hydraulic properties of the rock units shown in Figure 3 are given in Chapter 3 of Campbell, et al. [1978]. These are the properties of real rocks

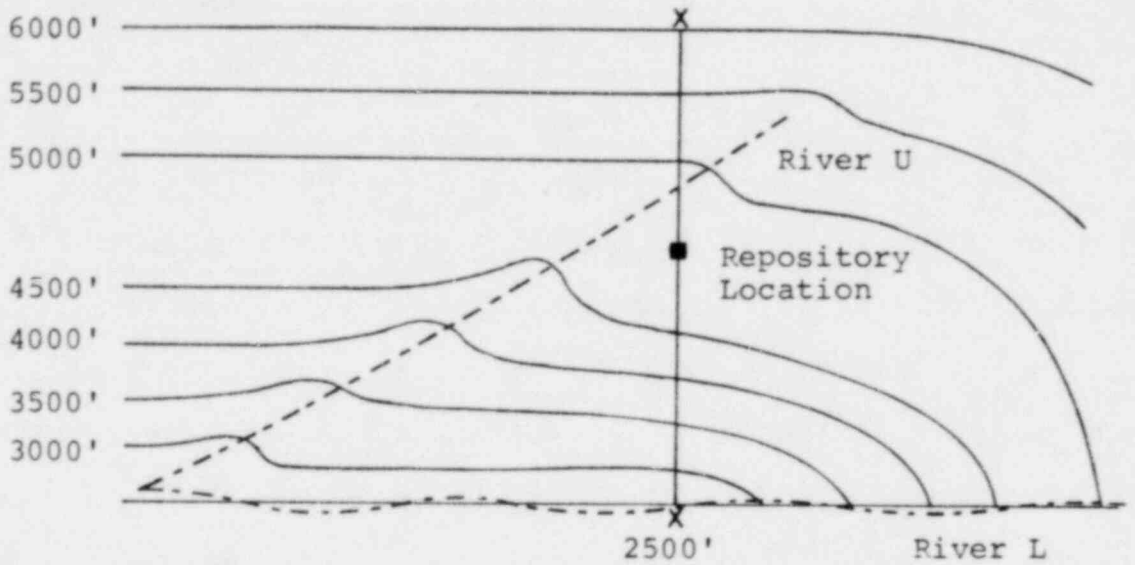

Figure 2. Physiographic Setting of the Reference Site.

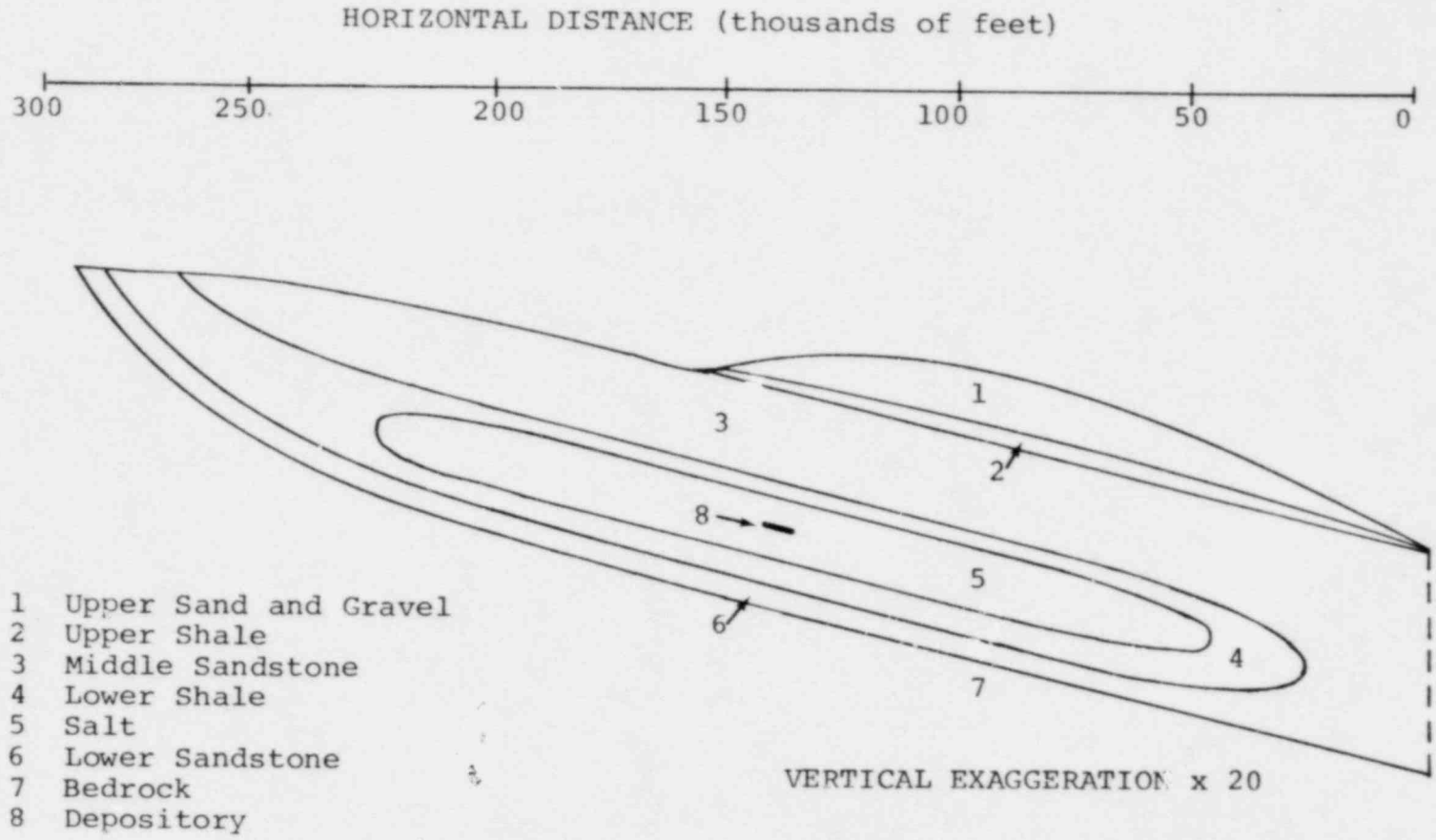

Figure 3. The Reference Site Geology.

[Franke and Cohen, 1972] with exception of the salt bed, whose hydraulic properties are not well known. There, the hydraulic conductivity and porosity of salt were arbitrarily assumed to be factors of 10^3 and 10 lower, respectively, than those of the shale bed.

The location of the repository, as may be inferred from the elevation contours of Figure 2, is far enough from the head of the valley that groundwater flow around the repository is perpendicular to River L and to the valley axis. Thus the SWIFT model may be used in its two-dimensional mode to simulate conditions around the repository.

Groundwater flow at the reference site has been simulated using the SWIFT model. The hydraulic head distribution is shown in Figure 4. The head distributions in the lower and middle sandstone aquifers (also referred to as underlying and overlying aquifers) indicate that flow in these aquifers is essentially one-dimensional. Furthermore, there is a downward gradient across the depository so that, should a hydraulic connection be established between the overlying and underlying aquifers, fluid flow would be downward. Darcy velocities, as calculated by the SWIFT model, are shown in Figure 5. The one-dimensional nature of fluid flow in the aquifers is clearly shown in this figure. Darcy velocities below 10^{-5} ft/day were not plotted which explains why no vectors are shown in the salt layer.

In this report, three scenarios are considered. These are: (1) a U-tube connecting the depository to the overlying aquifer

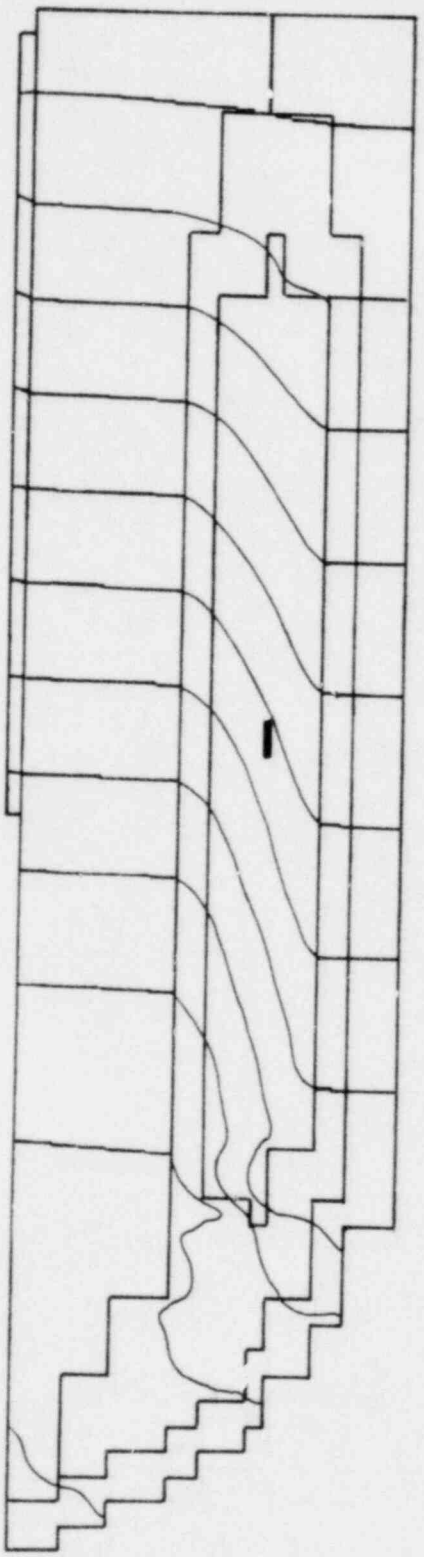

Figure 4. Pressure Head Distribution at the Reference Site.

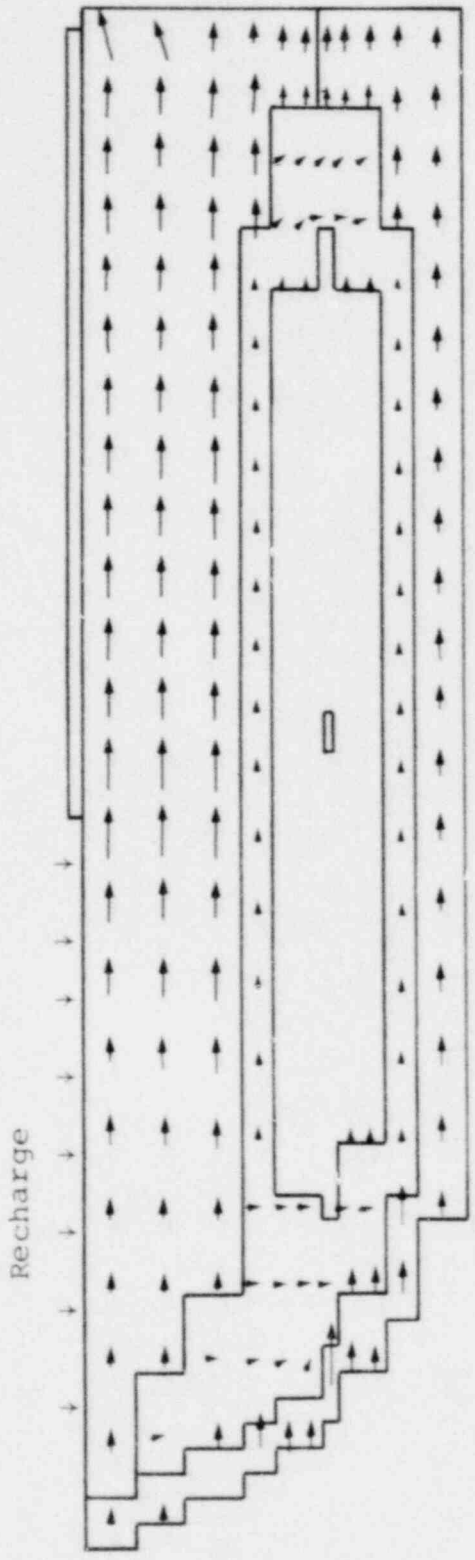

Figure 5. Darcy Velocity Vectors at the Reference Site.

with radionuclide discharge at River L, (2) a U-tube to the overlying aquifer with radionuclide discharge at a nearby well and (3) a hydraulic connection between the overlying and underlying aquifers passing through the depository with discharge at River L.

The U-tube, used in both scenarios 1 and 2, is assumed to result from seal failures of a shaft (30 feet in diameter) on the up-dip side of the depository and of a borehole (3 feet in diameter) on the down-dip side of the depository. The shaft, for example, could be a man-materials connection to the surface, and the borehole could be a ventilation pipe. The U-tube is included because it provides a hydraulic connection between the depository and the overlying aquifer and is, therefore, somewhat representative of a class of disruptive features which could provide such a hydraulic connection. The U-tube scenarios are shown in Figure 6. The shaft and borehole are not extended through the upper shale and upper sand and gravel layers because vertical hydraulic gradient between the middle sandstone and these layers is insignificant.

Fluid flow calculations have been performed with SWIFT to illustrate the effects of such a disruption on the flow system near the depository. The results are shown in Figure 7 where the Darcy velocity field is plotted. The effect of the disruptive feature is to allow water from the overlying aquifer to pass down through the depository then return to the aquifer. Thus, for this type of disruptive feature, the radionuclide migration path is along the overlying aquifer. It is interesting to note that the fluid flow in the overlying aquifer near the depository remains

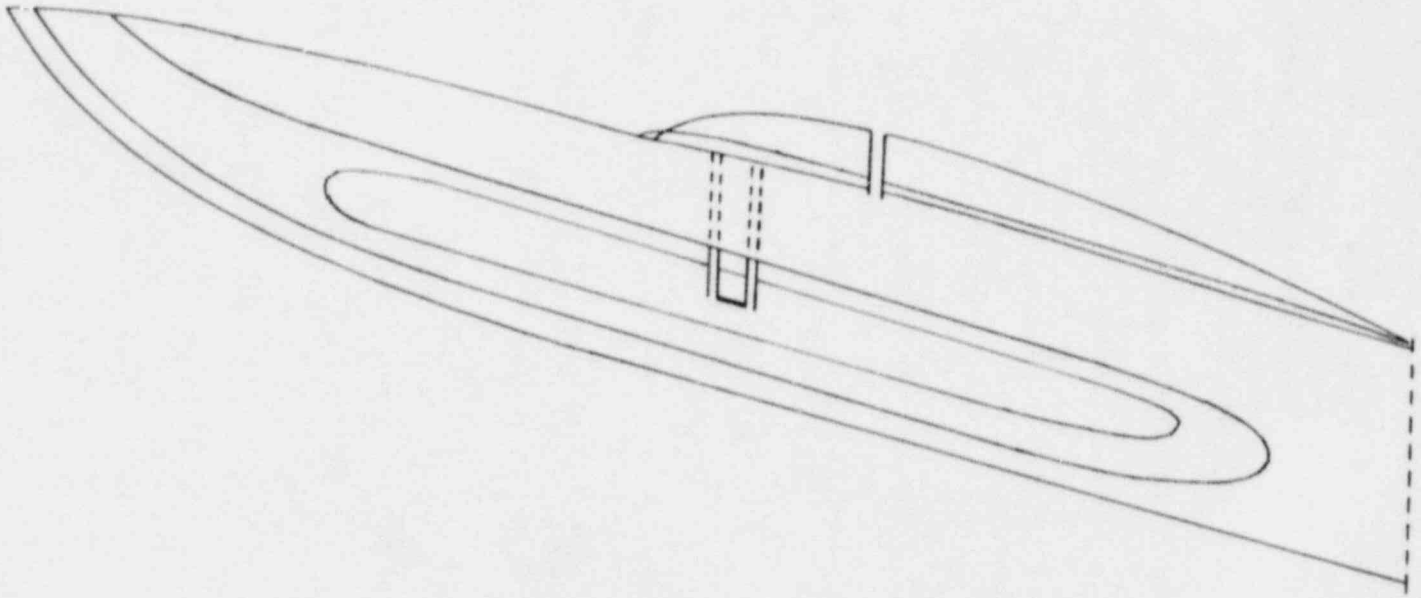

Figure 6. U-Tube Formed Through Depository. The Water Well in the Overlying Aquifer is Used in Scenario 2.

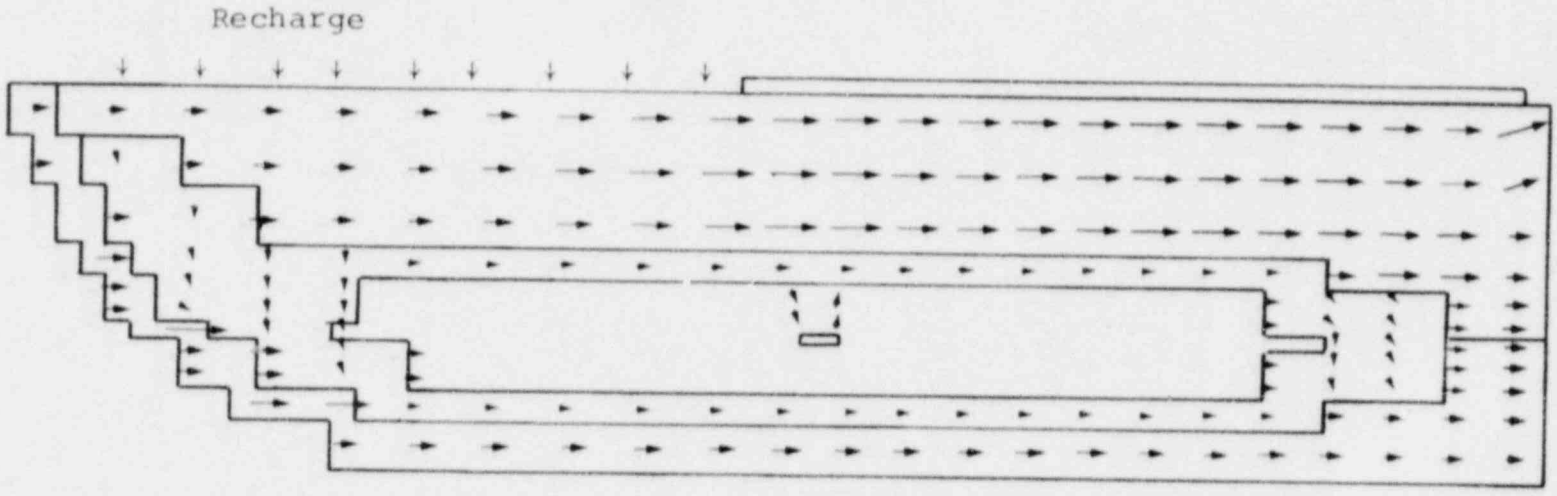

Figure 7. Darcy Velocity Field for a U-Tube Scenario.

essentially one-dimensional despite the presence of the disruptive feature.

Scenario 3 (hydraulic connection between the overlying and underlying aquifers) could result from exploratory drilling or faulting through the depository. In the present example, we have simply extended a 3 foot borehole through the depository. This scenario is shown in Figure 8. Results of flow calculations for this scenario are shown in Figure 9. As indicated by the Darcy velocity vectors, the radionuclide migration path is along the underlying aquifer to River L.

IV. COMPARISON OF SWIFT AND NWFT FOR A U-TUBE SCENARIO

As demonstrated above, numerical simulations have been carried out for the full two-dimensional system of Figure 3. Some selected three-dimensional systems in the near field of the depository have also been modeled using the SWIFT computer code. For the sensitivity analysis, however, a simplified one-dimensional representation of the full system and the U-tube was used. Fluid flow in the simplified system was established using pressure boundary conditions taken from a full-system simulation, and radionuclides were introduced into the system from an assumed inventory and leach rate or solubility limit.

As indicated in the introduction, fluid flow and radionuclide transport are controlled by hydrological and geochemical variables whose values are not generally well known for any given site. Because the reference site is hypothetical, measured data are not

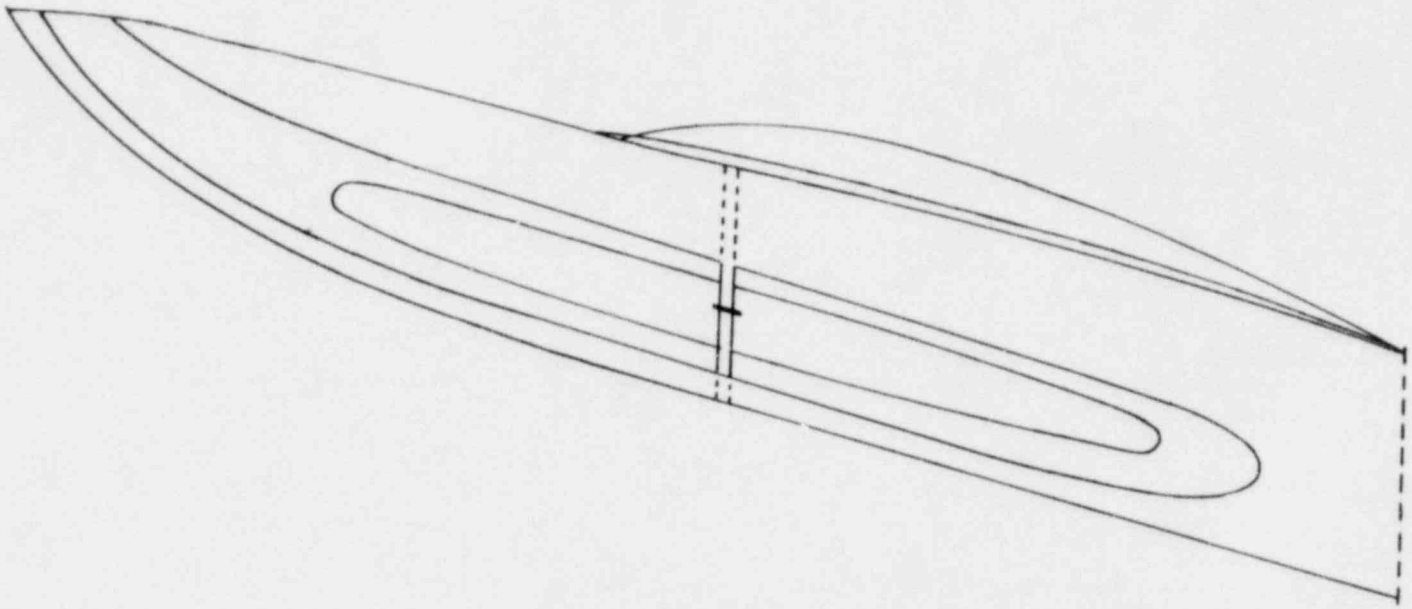

Figure 8. U-Tube Formed Through Depository.

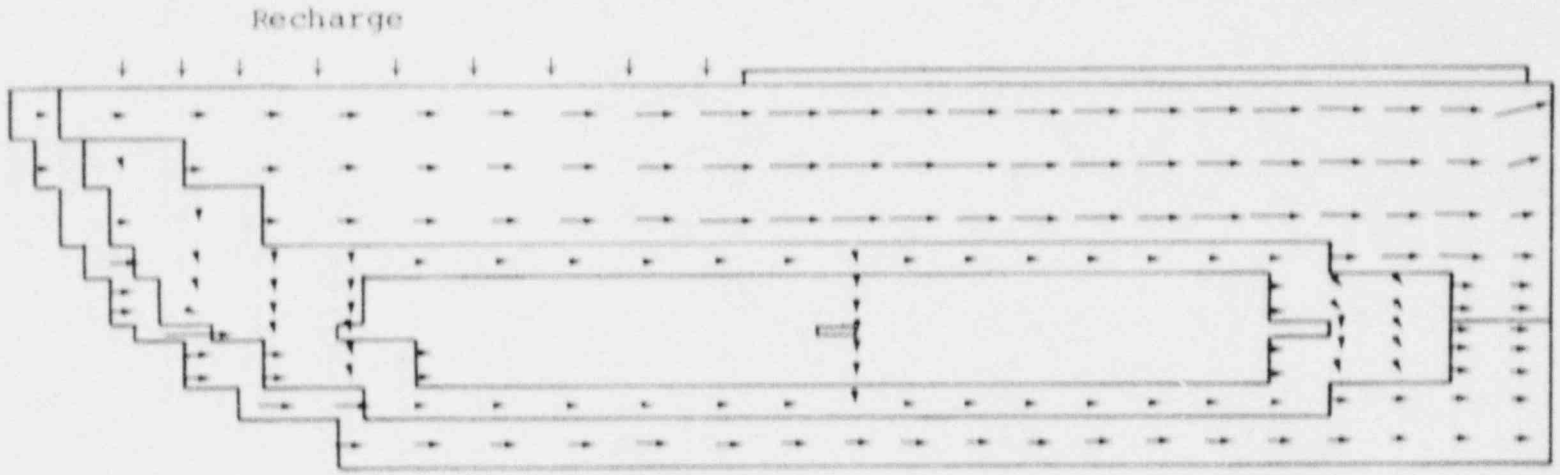

Figure 9. Darcy Velocity Field for a Hydraulic Connection Between the Overlying and Underlying Aquifers.

available for its hydrological and geochemical properties. Earth scientists from Sandia Laboratories, the U.S. Geological Survey and INTERA Environmental Consultants provided ranges and distributions for the site properties required in this study. The results of this effort are shown in Table 1 for the simplified U 238 chain, U 238 → U 234 → Th 230 → Ra 226. The ranges chosen are global in nature and, as such, are broader than one might reasonably expect for a particular site.

4.1 Sensitivity-Analysis Results for the SWIFT Model

Latin Hypercube Sampling was used to form 50 input vectors for the input variables listed in Table 1. SWIFT calculations were performed to determine time-dependent discharge rates to the environment at River L for U238, U234, Th230 and Ra226 for each of the 50 input vectors. Both peak discharge rate and total discharge (integrated to 10^6 years) were determined. Two stepwise regression analyses on ranks were performed using peak discharge rate and total discharge as dependent variables. Independent variables used in the analyses are shown in Table 2. Important variables selected by stepwise rank regression on peak discharge rate and total discharge were practically identical and, therefore, only results for total discharge are presented.

Important variables, as selected by stepwise rank regression analysis, are listed in Table 3. For U238 and U234, the uranium retardation factor in the shaft is the dominant variable whereas for Th230 and Ra226, the thorium and radium retardation factors in the aquifer are the most important variables. Recall that for

Table 1. Variable Ranges and Distributions

Variable*	Range	Distribution
ϕ_s	0.005 - 0.20	Log Normal
ϕ_a	0.05 - 0.30	Normal
K_s	0.01 - 50 ft/d	Log Normal
K_a	1.0 - 50 ft/d	Log Normal
α	45 - 500 ft	Uniform
k_d(U)	10^{-2} - 10^5 cm^3/g	Log Uniform
k_d(Th)	10^{-2} - 10^5 cm^3/g	Log Uniform
k_d(Ra)	10^{-2} - 10^3 cm^3/g	Log Uniform
τ	10^3 - 10^7 y	Log Uniform

*Variable Definitions:

ϕ = porosity, K = hydraulic conductivity, α = dispersivity, k_d = distribution coefficient, τ = leach time for a constant leach rate model.

Subscript Definitions:

s = shaft, a = aquifer.

Table 2. Independent Variables Used in Sensitivity Analysis

Variable	Description
$X_1 = 1/\phi_a$	Reciprocal of porosity in aquifer
$X_2 = K_a$	Hydraulic conductivity in aquifer
$X_3 = \alpha$	Dispersivity
$X_4 = 1/R_{U,a}$	Reciprocal of uranium retardation factor in aquifer
$X_5 = 1/R_{U,s}$	Reciprocal of uranium retardation factor in shaft
$X_6 = 1/R_{Th,a}$	Reciprocal in thorium retardation factor in aquifer
$X_7 = 1/R_{Th,s}$	Reciprocal of thorium retardation factor in shaft
$X_8 = 1/R_{Ra,a}$	Reciprocal of radium retardation factor in aquifer
$X_9 = 1/R_{Ra,s}$	Reciprocal of radium retardation factor in shaft
$X_{10} = 1/\tau$	Reciprocal of leach time for a constant leach rate source
$X_{11} = 1/\phi_s$	Reciprocal of porosity in shaft
$X_{12} = K_s$	Hydraulic conductivity in shaft
$X_{13} = K_a/\phi_a$	Hydraulic conductivity divided by porosity in aquifer
$X_{14} = K_s/\phi_s$	Hydraulic conductivity divided by porosity in shaft

Squares of all the above variables were included as well as physically reasonable cross-products.

Table 3. Important Variables from the SWIFT Sensitivity Analysis

Nuclide	Variables Selected	Standardized Regression Coefficients (Ranks)	R^2*	N
U238	$X_5 = 1/R_{U,s}$	1.94		
	$X_5^2 = 1/R_{U,s}^2$	-1.27		
	$X_{10}X_{14} = K_s/\phi_s$	0.24	0.789	30
U234	$X_5 = 1/R_{U,s}$	1.59		
	$X_5^2 = 1/R_{U,s}^2$	-0.84		
	$X_{10}X_{14} = K_s/\phi_s$	0.39	0.815	28
Th230	$X_6 = 1/R_{Th,a}$	0.90		
	$X_{10}X_{14} = K_s/\phi_s$	0.26	0.874	39
Ra226	$X_8 = 1/R_{Ra,a}$	0.65		
	$X_9X_{12} = K_s/R_{Ra,s}$	0.28	0.685	47

*R^2 = Ratio of the regression sum of squares to the total sum of squares.

N = Number of calculations giving non-zero discharge.

a given element, the same distribution coefficient is used for both the shaft and the aquifer in this analysis so that the only difference in retardation factors for the two portions of the system is the difference introduced by porosity variations. Therefore the shaft retardation factor is highly correlated with the aquifer retardation factor for any particular element. For this reason, the fact that the shaft retardation factor is selected for uranium while aquifer retardation factors are selected for thorium and radium is probably not significant. Such results simply emphasize the importance of the distribution coefficient.

For U238, U234 and Th230, the reciprocal of the leach time (X_{10}) enters in combination with the ratio of hydraulic conductivity to porosity (X_{14}) in the shaft. In this case, variable X_{10} is highly correlated with variable $X_{10} * X_{14}$. Hence, even though the regression analysis selected the product $X_{10} * X_{14}$, this may only indicate the importance of the leach time. Stepwise rank regression on the integrated discharge for Ra226 selected the radium retardation factor for the aquifer (X_8) and the product of the retardation factor for the shaft with the hydraulic conductivity for the shaft ($X_9 * X_{12}$). The reason that the leach time does not appear for radium is that Ra226 has a relatively short (1600y) half life so that most of the radium discharged is produced by decay of Th230.

As stated earlier, the primary purpose of the analysis presented here is to study the relative importance of hydraulic and geochemical variables which control radionuclide migration in groundwater. Thus, while stepwise regression is central to the

determination of variable importance, the response surface itself is not necessarily an important product of the analysis. However, to provide confidence that the variables selected by the regression analysis are indeed the most important ones, it is important to assure that the fitted response surface adequately predicts the original SWIFT output. Comparisons between the original SWIFT output and the predicted output from the fitted response surface are provided by the cumulative distributions in Figure 10. For all four isotopes, the fitted response surface adequately reproduces the cumulative distribution function determined from the SWIFT results.

4.2 Sensitivity-Analysis Results for the NWFT Model

The Network Flow and Transport (NWFT) Model has been developed at Sandia to provide a simple, efficient capability for calculating radionuclide migration in groundwater [Campbell, et al., 1979]. The network flow system utilized in NWFT is shown in Figure 11. Fluid discharge and velocity are determined by requiring conservation of mass at the segment junctions. Once the flow system is established, the radionuclide migration pathway from the depository to the discharge point is determined. Radionuclide discharge is then calculated by assuming that transport occurs along a single, one-dimensional path having length equal to the total migration path length and by using the average isotope velocity. In its present form, NWFT will transport a chain of no more than three isotopes which are required to have the same distribution coefficient.

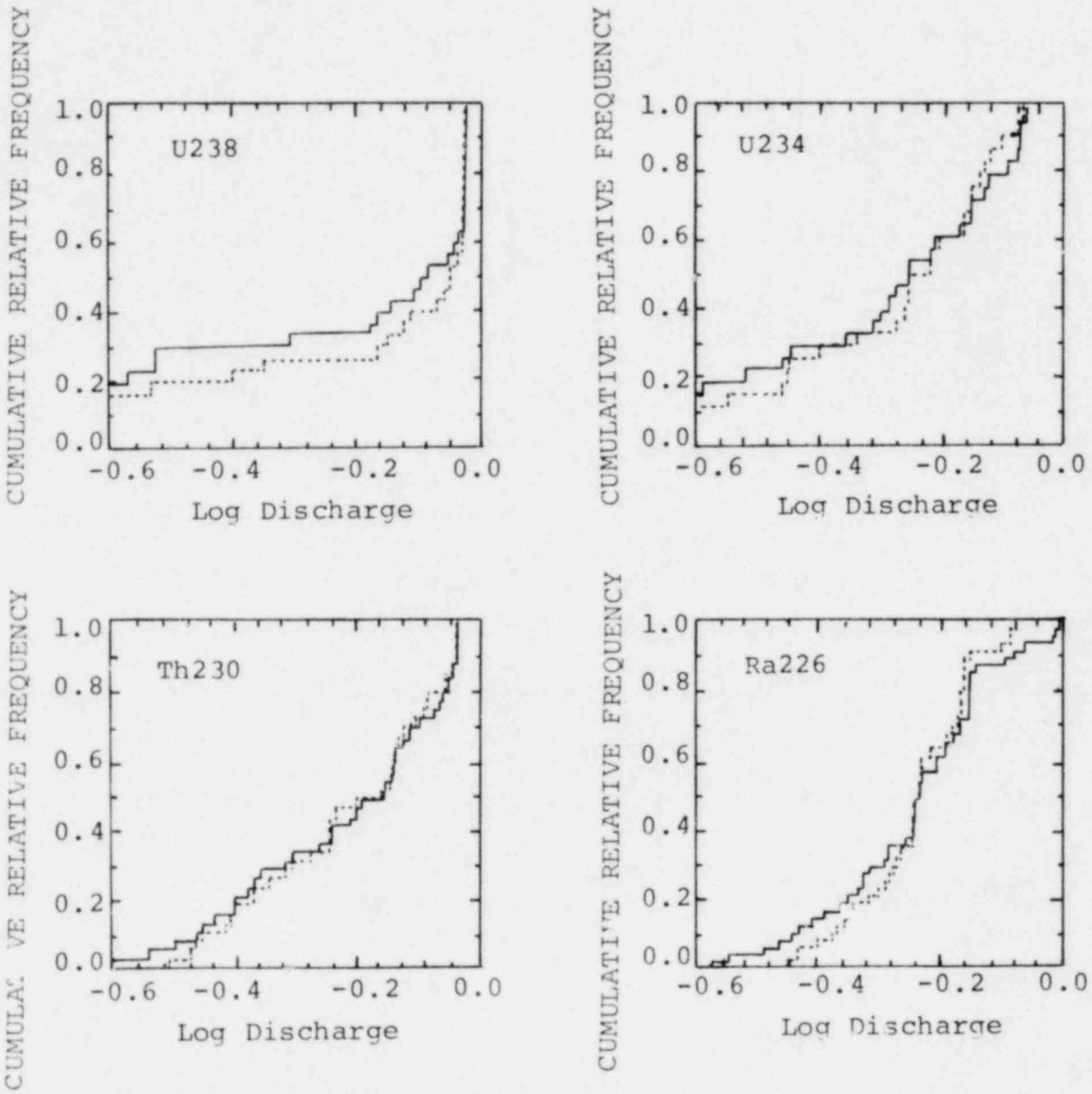

Figure 10. Comparisons Between SWIFT Results and the Response Surfaces Fitted to Nonzero Results. All Discharge Results Normalized to Maximum Observed Discharge. Solid lines are used for SWIFT results. Dashed lines are used for response surface results.

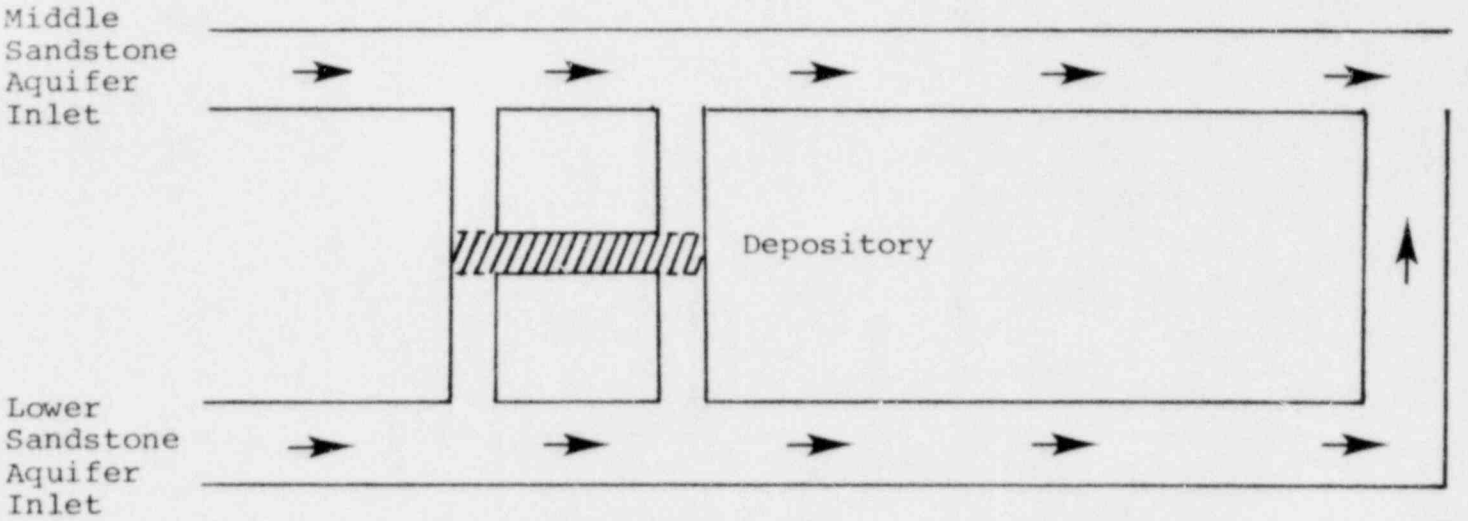

Figure 11. Network Representation of Reference Site Flow System.

NWFT was used to represent the reference site and disruptive event described in Chapters III and IV to determine whether such a simple model could be used to perform meaningful sensitivity studies. Pressure boundary conditions for NWFT were taken from a two-dimensional SWIFT flow calculation for the full reference system. The same 50 input vectors used in the SWIFT sensitivity analysis were then input to NWFT to determine integrated radionuclide discharge. As NWFT requires all isotopes to have the same distribution coefficient, only U238 and U234 were transported. Important variables selected by stepwise regression on ranks are shown in Table 4.

The variables selected from the NWFT sensitivity analysis are identical to those selected in the SWIFT sensitivity analysis (Table 3) with the exception that leach time appeared alone in the NWFT analysis whereas it appeared in combination with the ratio of hydraulic conductivity to porosity for the shaft in the SWIFT analysis.

Comparisons of cumulative distribution functions for total discharge between SWIFT and NWFT are shown in Figures 12 and 13. Differences between results for the two models can be explained by the fact that SWIFT introduces some numerical dispersion whereas NWFT, using an analytical expression for discharge, does not. Thus calculations which produce no discharge in NWFT may produce small discharge in SWIFT. Similarly, calculations which discharged the full radionuclide inventory in NWFT may discharge slightly less than the full inventory in SWIFT. Our conclusion,

Table 4. Important Variables Selected for the NWFT Analyses

Nuclide	Variables Selected	Standardized Regression Coefficients (Ranks)	R^{2}*	N
U238	$X_5 = 1/R_{U,s}$	1.55		
	$X_5^2 = 1/R_{u,s}^2$	-1.06		
	$X_{10} = 1/\tau$	0.73	0.666	30
U234	$X_5 = 1/R_{U,s}$	1.74		
	$X_5^2 = 1/R_{U,s}^2$	-1.21		
	$X_{10} = 1/\tau$	0.69	0.833	30

---

*R^2 = Ratio of the regression sum of squares to the total sum of squares.

N = Number of calculations giving non-zero discharge.

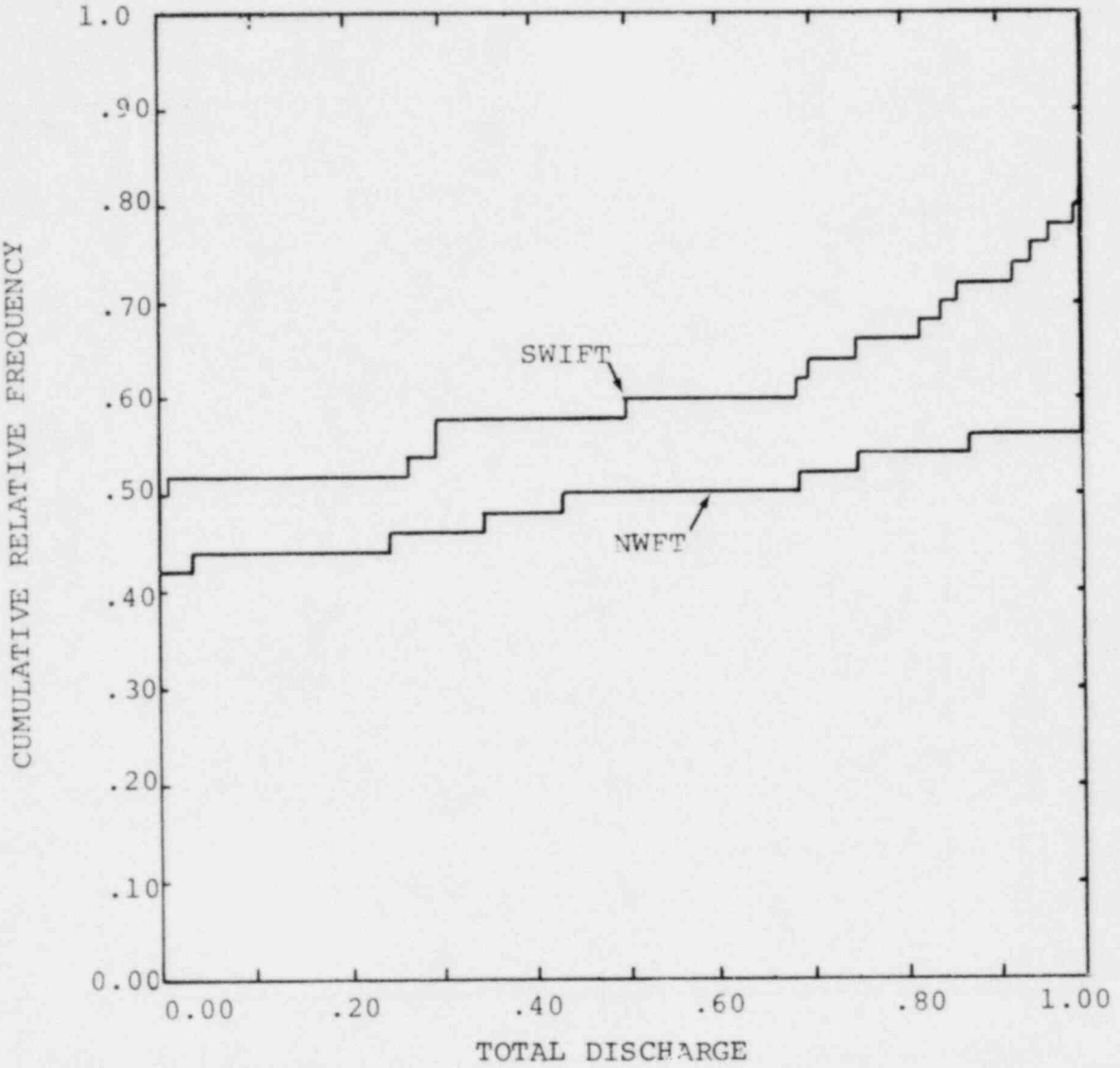

Figure 12. Comparison of SWIFT and NWFT Cumulative Relative Frequency Distributions for U238. Discharge Results Normalized to Maximum Observed Discharge.

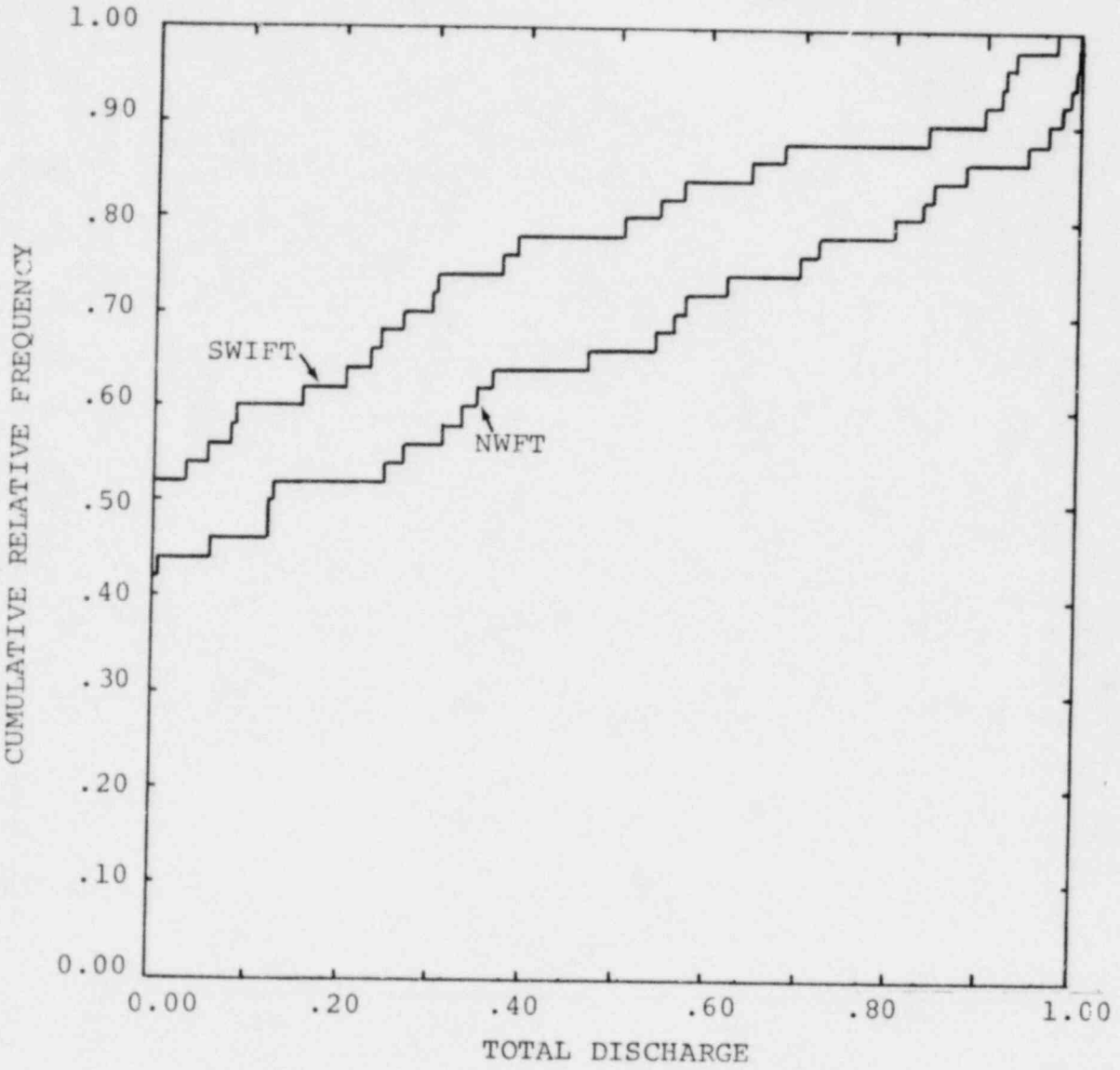

Figure 13. Comparison of SWIFT and NWFT Cumulative Relative Frequency Distributions for U234. Discharge Results Normalized to Maximum Observed Discharge.

based on comparisons of variable selections and cumulative distributions, is that NWFT may be used to perform meaningful sensitivity analysis. Results in the remainder of this report were produced with NWFT.

V. ADDITIONAL SCENARIO STUDIES

In this chapter, the three scenarios described in Chapter III are evaluated. These scenarios are: (1) U-tube with radionuclide discharge at River L, (2) U-tube with radionuclide discharge at a nearby well and (3) a hydraulic connection between the overlying and underlying aquifers passing through the depository with discharge at River L. The NWFT model is used in all calculations. Four nuclides are considered with half lives that vary from 10^3 to 10^6 years to examine the effect of half life on discharge and variable importance. An initial inventory of 1000 Ci is assumed for each nuclide. Input variables ranges and distributions are shown in Table 5. These ranges and distributions are the same as found in Table 1 for uranium except that a solubility limit has been added. The same basic variable ranges and distributions are used for all four nuclides. The dependent variables in all cases is the total discharge integrated to 10^6 years. Independent variables used in these analyses are shown in Table 6.

5.1 Theoretical Development

To aid understanding of the results presented in the remainder of this chapter, it will be useful to briefly review analytical expressions for one-dimensional transport of radionuclides. The

Table 5. Variable Ranges and Distributions

Variable*	Range	Distribution
ϕ_s	0.003 - 0.20	Log Normal
ϕ_a	0.05 - 0.30	Normal
K_s	0.01 - 50 ft/d	Log Normal
K_a	1.0 - 50 ft/d	Log Normal
α	45 - 500 ft	Uniform
k_d	10^{-2} - 10^{5} cm^3/g	Log Uniform
τ	10^{3} - 10^{7} y	Log Uniform
C	10^{-12} - 10^{-6}	Log Normal

*Variable Definitions:

ϕ = porosity, K = hydraulic conductivity, α = dispersivity, k_d = distribution coefficient, τ = leach time for a constant leach rate source model, C = solubility limit

Subscript Definitions:

s = shaft, a = aquifer

Table 6. Independent Variables Used in Sensitivity Analysis

Variable	Description
$X_1 = 1/\phi_a$	Reciprocal of porosity in aquifer
$X_2 = K_a$	Hydraulic conductivity in aquifer
$X_3 = \alpha$	Dispersivity
$X_4 = 1/R_a$	Reciprocal of retardation factor in aquifer
$X_5 = 1/R_s$	Reciprocal of retardation factor in shaft
$X_6 = C$	Radionuclide solubility limit
$X_7 = 1/\phi_s$	Reciprocal of porosity in shaft
$X_8 = K_s$	Hydraulic conductivity in shaft
$X_9 = 1/\tau$	Reciprocal of leach time for a constant leach rate source
$X_{10} = 1/k_d$	Reciprocal of distribution coefficient

Squares of all the above variables were included as well as physically reasonable cross products.

equation describing one-dimensional migration of the i^{th} isotope in a radioactive decay chain is [Burkholder and Rosinger, 1980]:

$$R_i \frac{\partial C_i}{\partial t} + v \frac{\partial C_i}{\partial z} = D \frac{\partial^2 C_i}{\partial z^2} - R_i \lambda_i C_i + R_{i-1} \lambda_{i-1} C_{i-1} \qquad (1)$$

where $R_i = 1 + \frac{k_{di} \rho}{\phi}$ = retardation factor for isotope i

kd_i = distribution coefficient for isotope i

ρ = rock bulk density

ϕ = porosity

C_i = concentration of isotope i in fluid

v = interstitial fluid velocity

$D = \alpha |v|$ = dispersion coefficient

α = dispersivity

λ_i = decay constant for isotope i

z = distance from source

t = time

For a single isotope and a constant leach rate source, appropriate boundary conditions are

$$\left.\begin{array}{l} t = 0 \\ z \geq 0 \end{array}\right\} \quad C = 0$$

$$\left.\begin{array}{l} 0 < t \leq \tau \\ z = 0 \end{array}\right\} \quad C = \frac{I}{Q\tau} e^{-\lambda t}$$

$$\left.\begin{array}{l} t > \tau \\ z = 0 \end{array}\right\} \quad C = 0$$

$$\left.\begin{array}{l} t > 0 \\ z \to \infty \end{array}\right\} \quad C = \text{finite}$$

where τ = leach time for a constant leach rate source

Q = fluid flow at source

I = initial quantity of isotope

The solution of equation (1), subject to the boundary conditions stated above, is

$$C(z,t) = \frac{I}{Q\tau} e^{-\lambda t} \left[G(t) - G(t - \tau)\, S(t - \tau)\right] /2 \qquad (2)$$

where the functions G and S are defined by

$S(x) = 0 \qquad x < 0$

$S(x) = 1 \qquad x \geq 0$

$$G(t) = \text{erfc} \frac{z-vt}{\sqrt{4\alpha vt}} + e^{z/\alpha} \text{erfc} \frac{(z+vt)}{\sqrt{4\alpha vt}}$$

erfc = complementary error function

For the no dispersion case ($\alpha = 0$), the solution to equation (1) is

$$C(z,t) = \frac{I}{Q\tau} e^{-\lambda t} \left[S\left(\frac{v}{R} t - z\right) - S\left(\frac{v}{R} (t - \tau) - z\right)\right] \qquad (3)$$

If $z = L$ is the distance from the radionuclide source to a discharge point, then the rate of radionuclide discharge is

$$D(t) = Q\, C(L, t) \tag{4}$$

The no dispersion solution (equation 3) provides a useful example for examination of the effects on discharge rate of variables which control migration time and source rate. It can be seen from equations (3) and (4) that discharge only occurs for

$$\frac{RL}{v} \leq t < \frac{RL}{v} + \tau \tag{5}$$

The radionuclide migration time is

$$T = RL/v \tag{6}$$

Because of the exponential decay term in equation (3), the migration time strongly affects discharge rate and, therefore, total discharge for isotopes with half lives small compared to the migration time. On the other hand, discharge rate varies linearly with the leach rate $1/\tau$ (or more generally, the source rate). Furthermore, the duration of the discharge pulse and the time period over which radioactive decay can reduce the radionuclide inventory at the source is determined by the leach time. Thus one might expect the relative importance of migration time to be greater for isotopes with short half lives (short relative to migration time)

than for isotopes with long half lives. The relative importance of source rate, however, might be expected to increase for isotopes with long half lives.

For one-dimensional flow in a homogeneous medium, the interstitial fluid velocity is given by

$$v = \frac{Ki}{\phi} \tag{7}$$

where K = hydraulic conductivity

i = hydraulic gradient

Thus from equations (6) and (7),

$$T = \frac{R\phi L}{Ki} \tag{8}$$

In this study, the hydraulic gradient is determined by the geometrical arrangement, dip angle and hydraulic properties of the various rock units at the reference site. The migration path length is determined by the scenario under consideration. Thus the migration time will be determined by the retardation factors (or distribution coefficients), porosities and hydraulic conductivities of the rocks through which radionuclides migrate from the depository to the environment.

For a leach limited source, the source rate is entirely controlled by the leach rate ($1/\tau$). For a solubility limited source, the source rate is determined by

$$\text{Source rate} = CQ$$

where C = radionuclide solubility limit (mass radionuclide/ mass fluid)

Q = fluid flow rate (mass fluid/unit time)

Thus for the solubility limited case, the source rate is controlled by the radionuclide solubility limit and by the hydraulic properties of the flow system in the vicinity of the depository.

5.2 U-Tube Scenario with Discharge at River L

The procedure here parallels that of the previous chapter. A total of 200 input vectors were obtained by Latin hypercube sampling on the indicated variable ranges. Two sets of NWFT calculations were then performed to determine the integrated discharge to River L for 10^6 years. In the first set of calculations, the radionuclide source rate was controlled by a leach rate. In the second set, the source rate was controlled by a solubility limit. For each set of calculations, NWFT runs were performed for each of the 200 input vectors and for each of four nuclides with half lives varying from 10^3 to 10^6 years. Stepwise regression on ranks was used to determine important variables. Results from the leach limited cases will be discussed first.

Leach Limitation. Cumulative frequency distributions for the leach-limited cases are shown in Figures 14 through 17. These figures indicate, as expected, that the total discharge generally increases as the nuclide half-life increases.

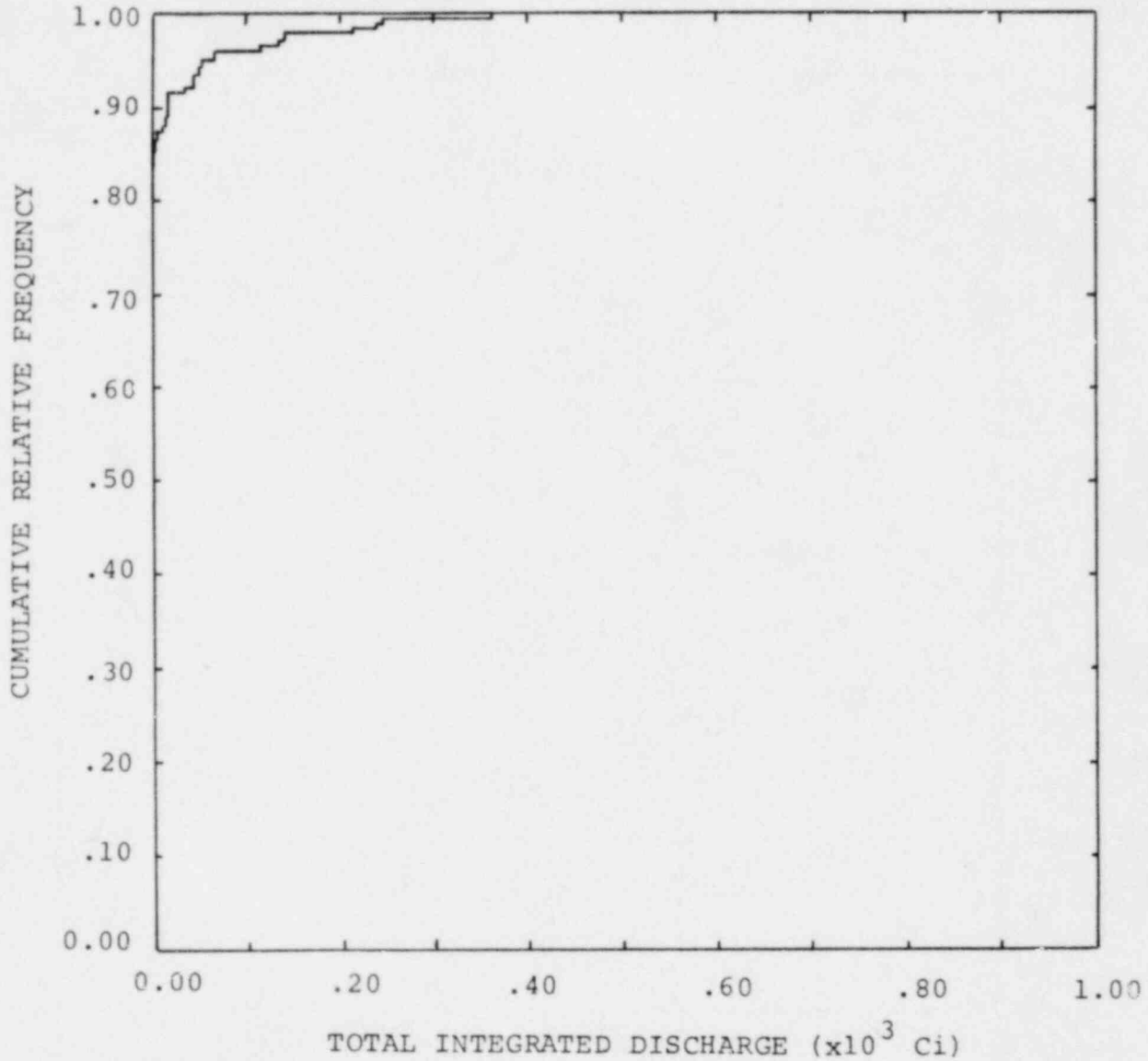

Figure 14. Cumulative Relative Frequency Distribution for Total Discharge at River L from the U-Tube Scenario with Leach-Limited Source. Radionuclide Half-Life is 10^3 Years.

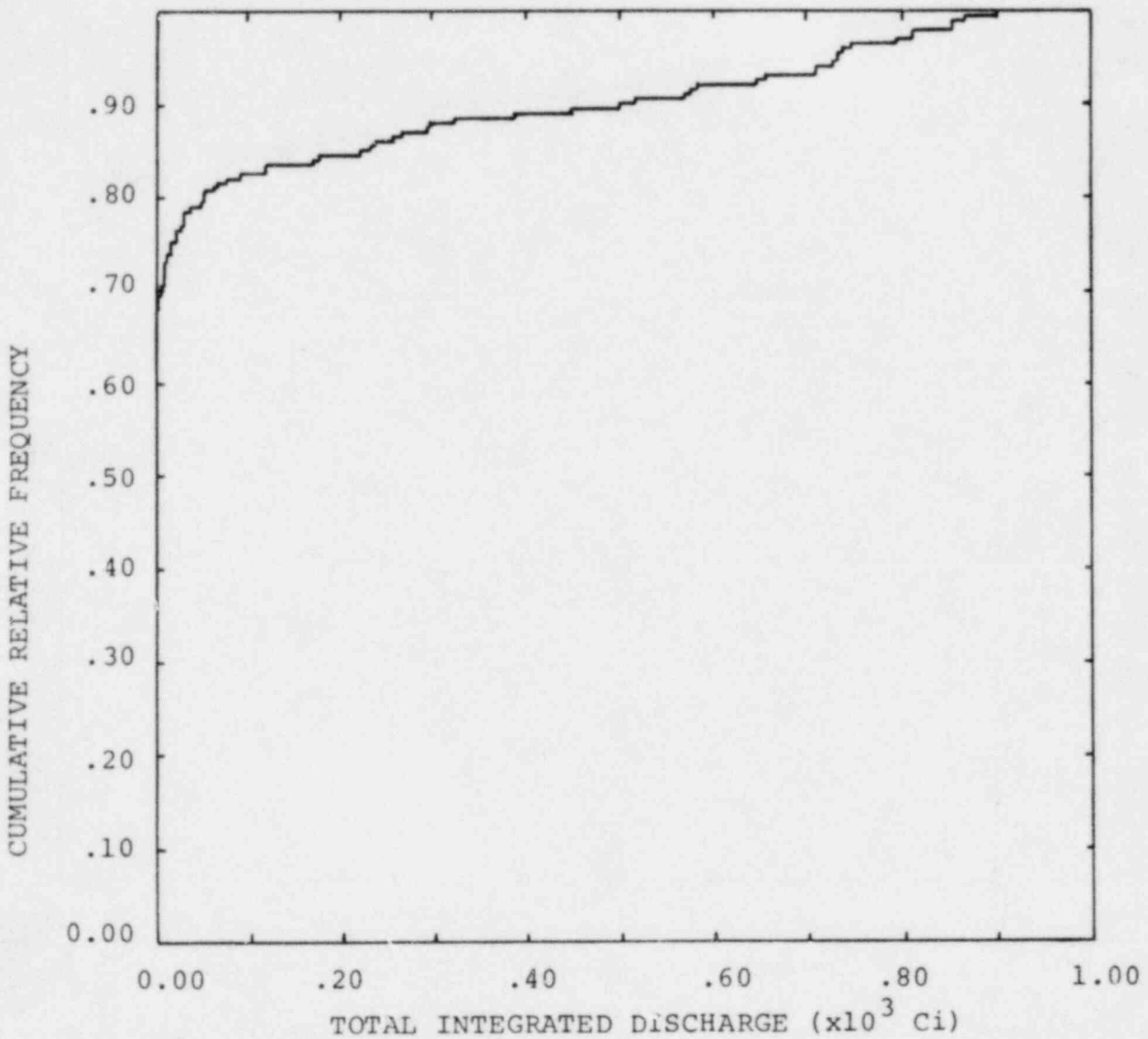

Figure 15. Cumulative Relative Frequency Distribution for Total Discharge at River L from the U-Tube Scenario with Leach-Limited Source. Radionuclide Half-Life is 10^4 Years.

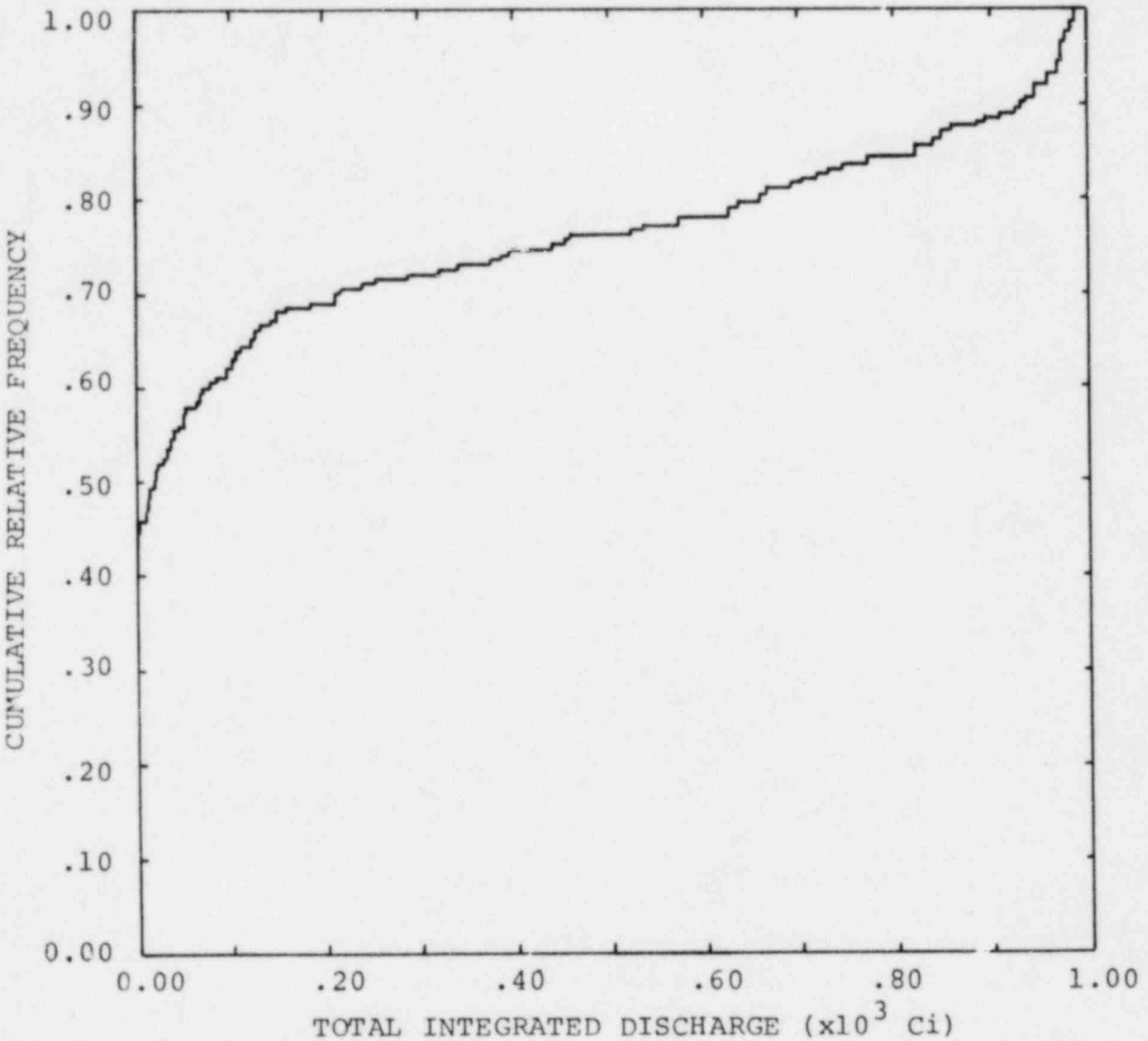

Figure 16. Cumulative Relative Frequency Distribution for Total Discharges at River L from the U-Tube Scenario with Leach-Limited Source. Radionuclide Half-Life is 10^5 Years.

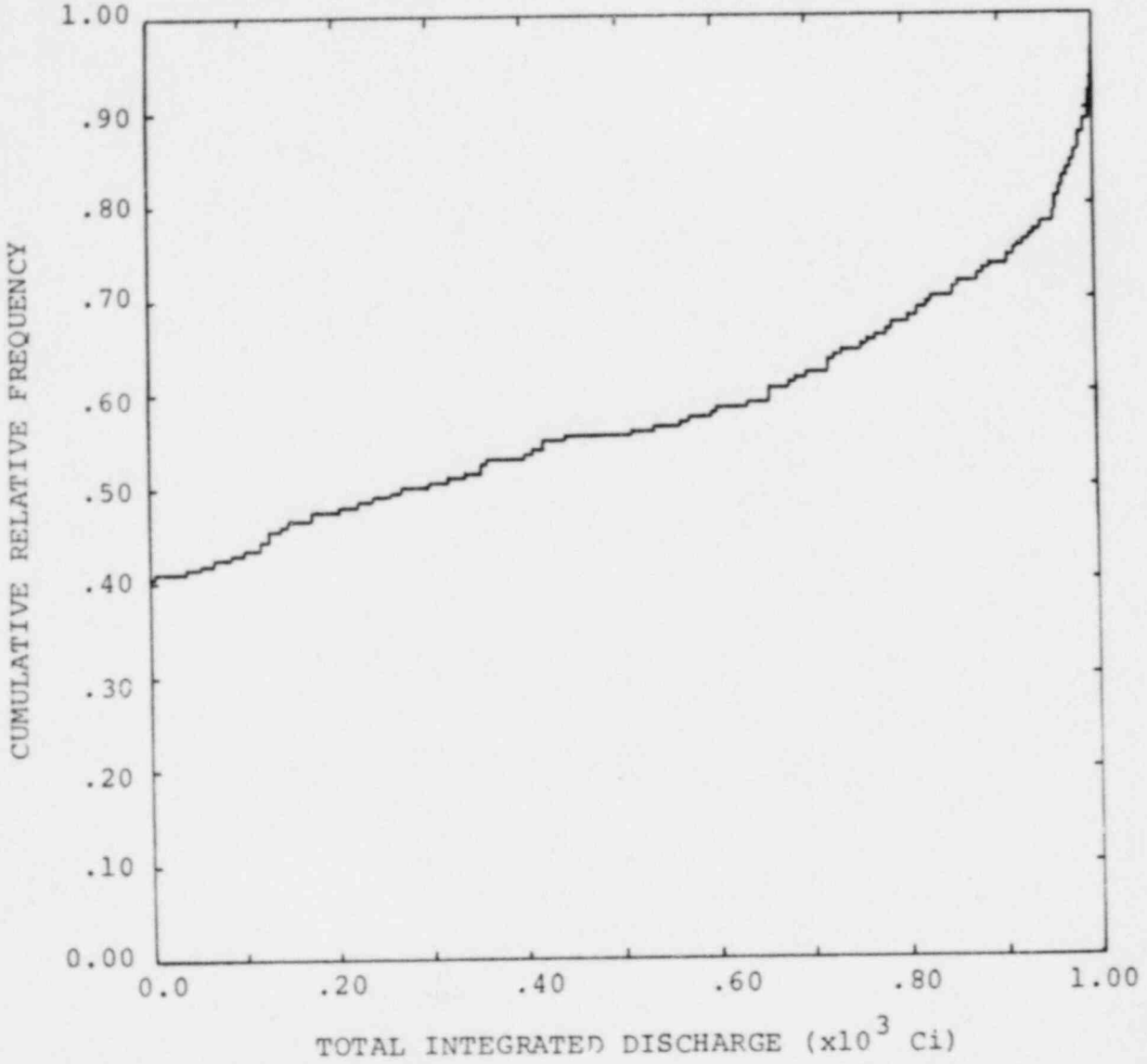

Figure 17. Cumulative Relative Frequency Distribution for Total Discharge at River L from the U-Tube Scenario with Leach-Limited Source. Radionuclide Half-Life is 10^6 Years.

Important variables, as selected by stepwise regression on ranks, are shown in Table 7. Also shown there are the standardized regression coefficients on ranks and the R^2 values. The absolute value of the former quantity provides a relative ordering of each variable. The latter quantity assumes values from zero to one which, when multiplied by 100, indicates the percent of variation in the total discharge which is explained by the accompanying variables.

For all half lives considered, the distribution coefficient or the aquifer retardation factor (k_d) appears as the most important variable. As indicated in the previous chapter, the same value of k_d is used in both the borehole and the aquifer. Thus the distribution coefficient, the borehole retardation factor and the aquifer retardation factor are all highly correlated. The selection of any of these three variables as important simply indicates the importance of the distribution coefficient.

Two possible trends seem to be indicated in Table 7. First, the quality of the response surface fit, as measured by R^2, improves as the half life increases. The reason for this improvement is that fewer runs result in zero discharge for the larger half lives. The second trend is that the leach time ($1/\tau$) appears to become more important for longer half lives.

To investigate the first apparent trend, zero values of discharge were excluded and then stepwise rank regression analysis was performed on the remaining, nonzero results. Important variables are shown in Table 8. The quantity N is the number of runs,

Table 7. Important Variables Selected by Stepwise Regression on Ranks for the U-Tube Scenario with Leach-Limited Source.

Half Life (years)	Variables Selected	Standardized Regression Coefficient	R^2
10^3	$(1/k_d)^2$	1.22	0.51
	$1/k_d$	-0.31	
	$K_a/(\phi_a\tau)$	0.13	
10^4	$1/R_a$	0.55	0.50
	$(1/R_a)^2$	0.37	
	$K_a/(\phi_a\tau)$	0.16	
10^5	$1/R_a$	0.88	0.70
	$1/\tau$	0.21	
	$(K_a/\phi_a)^2$	0.09	
	$1/\phi_s$	0.06	
10^6	$1/R_a$	1.13	0.82
	$1/\tau$	0.54	
	$(1/\tau)^2$	-0.30	
	$(1/R_s)^2$	-0.28	
	(K_a/ϕ_a)	0.10	

Table 8. Important Variables Selected by Stepwise Regression on Ranks for the U-Tube Scenario with Leach-Limited Source. Zero Discharges Excluded.

Half Life (years)	Variables Selected	Standardized Regression Coefficient	R^2	N
10^3	$1/k_d$	1.68	0.74	82
	$(1/k_d)^2$	-0.99		
	$(1/\tau)^2$	0.43		
	$K_s/(\phi_s\tau)$	0.22		
	K_a/ϕ_a	0.13		
10^4	$1/R_a$	1.88	0.89	111
	$(1/R_a)^2$	-1.22		
	$1/\tau$	0.52		
	$K_a/\phi_a\tau$	0.12		
10^5	$1/R_a$	1.88	0.92	126
	$(1/R_a)^2$	-1.25		
	$1/\tau$	0.45		
	$K_a/(\phi_a\tau)$	0.23		
10^6	$1/k_d$	1.67	0.76	126
	$(1/k_d)^2$	-1.66		
	$1/\tau$	1.33		
	$(1/\tau)^2$	-0.75		
	$K_a/(\phi_a\tau)$	0.17		

from the original 200, which produced nonzero discharge. Variables selected as important in this analysis are, for practical purposes, identical to results obtained when zero values are included. However, the quality of the response surface fit has generally improved as indicated by larger values of R^2.

Rank correlation coefficients with total discharge are used to illustrate the second trend indicated in Table 7; i.e., the dependence of input variable importance on radionuclide half-life. The rank correlation coefficients are calculated during the regression analysis. Rank correlation coefficients are plotted as a function of half life for variables $1/\tau$ and $1/k_d$ in Figure 18. The solid lines represent results where zero discharge cases are excluded. The dashed lines represent results where zero discharge cases are included. Although other variables (K_s, K_a, ϕ_s, ϕ_a) influence radionuclide migration time, the distribution coefficient, because of its large range, is the dominant variable controlling migration time. For the leach-limited case, the leach time ($1/\tau$) controls the source rate. The results shown in Figure 18 indicate that the importance of migration time (as represented by $1/k_d$) decreases with increasing half life whereas the importance of source rate (as represented by $1/\tau$) increases with increasing half life. When zero discharges are included, these trends are somewhat obscured.

Solubility Limitation. In this case, the radionuclide source rate is controlled by the solubility limit rather than by the leach rate. Cumulative frequency distributions for total discharge are

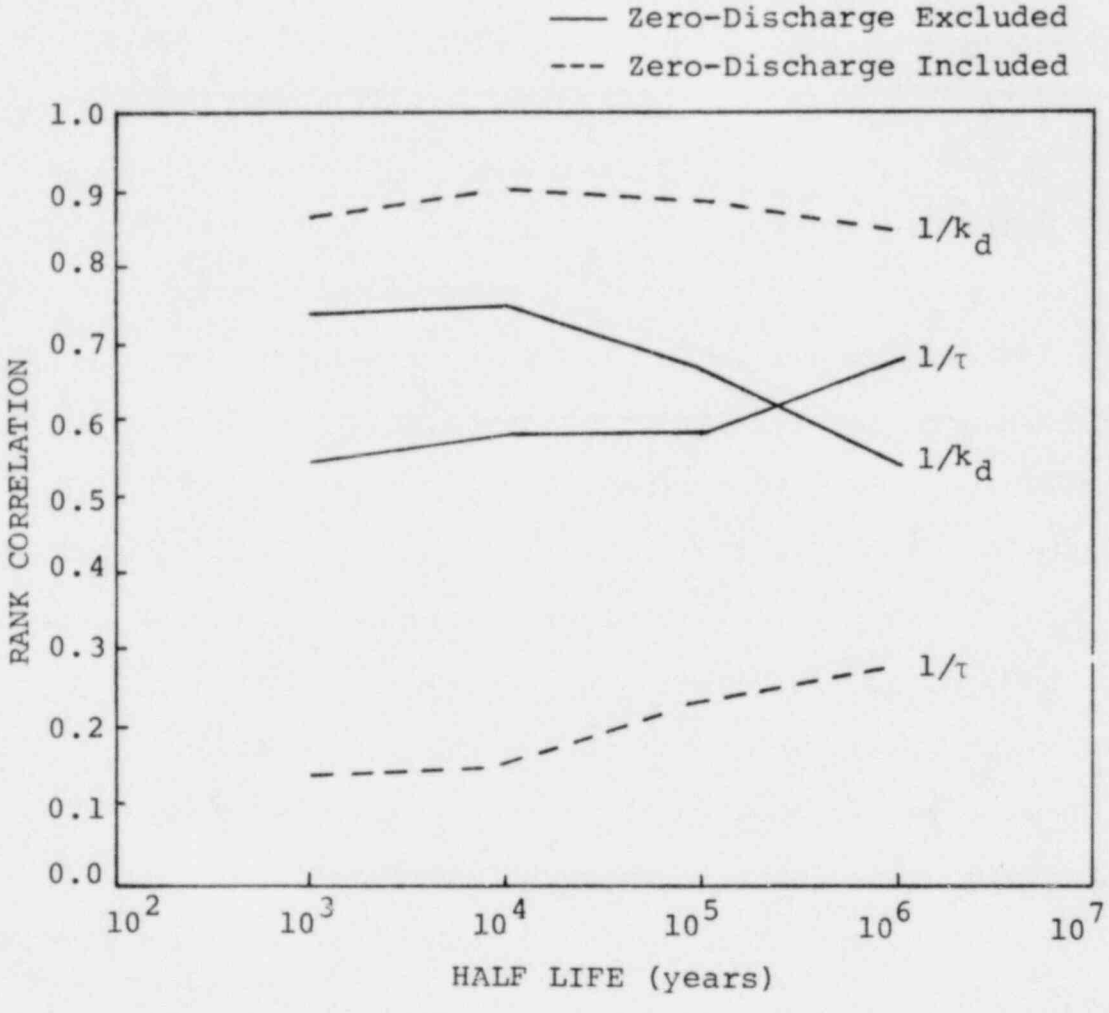

Figure 18. Rank Correlation Coefficients as a Function of Half-Life for $1/k_d$ and $1/\tau$. U-Tube Scenario with Leach-Limited Source.

shown in Figure 19 through 22. As in the leach-limited case, total discharge generally tends to increase as half life increases. However, the increase in total discharge with increasing half-life is not as pronounced as in the leach-limited case. In fact, Figures 21 and 22 indicate that, with the solubility-limited source, total discharge for 10^6 year half-life is generally lower than for 10^5 year half-life. These differences between leach- and solubility-limited cases can be explained as follows. For the leach-limited source, all radioactive material is released in a specified time (i.e., the leach time τ). Thus as half-life increases, the only effect is to reduce radioactive decay losses. For a solubility-limited source, there is a second effect which is important. The solubility-limit is expressed as mass of radionuclide per mass fluid. For a given solubility limit, a longer half-life implies a lower source rate in curies per unit mass of radioactive material. Therefore, for a solubility-limited source, increased half life tends to increase integrated discharge by decreasing decay losses but increased half-life also tends to decrease integrated discharge by reducing the specific activity of the radionuclide mass entering solution at the source.

Important variables, as selected by stepwise regression on ranks for the solubility limited case are shown in Table 9. The solubility limit plays essentially the same role here as the reciprocal of the leach time in the leach-limited cases. Otherwise there is no practical difference in the variables selected

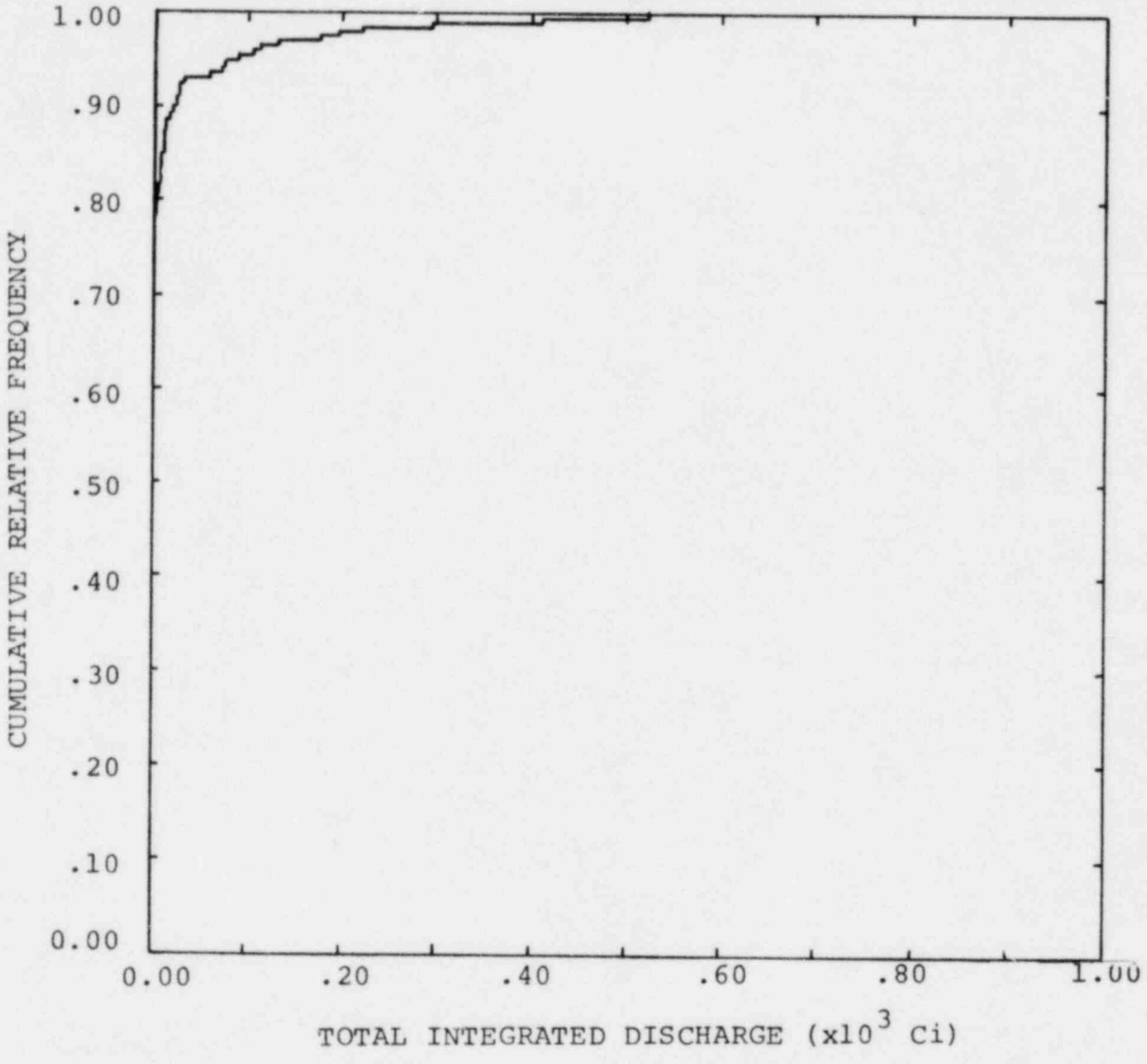

Figure 19. Cumulative Relative Frequency Distribution for Total Discharge at River L from the U-Tube Scenario with Solubility-Limited Source. Radionuclide Half-Life is 10^3 Years.

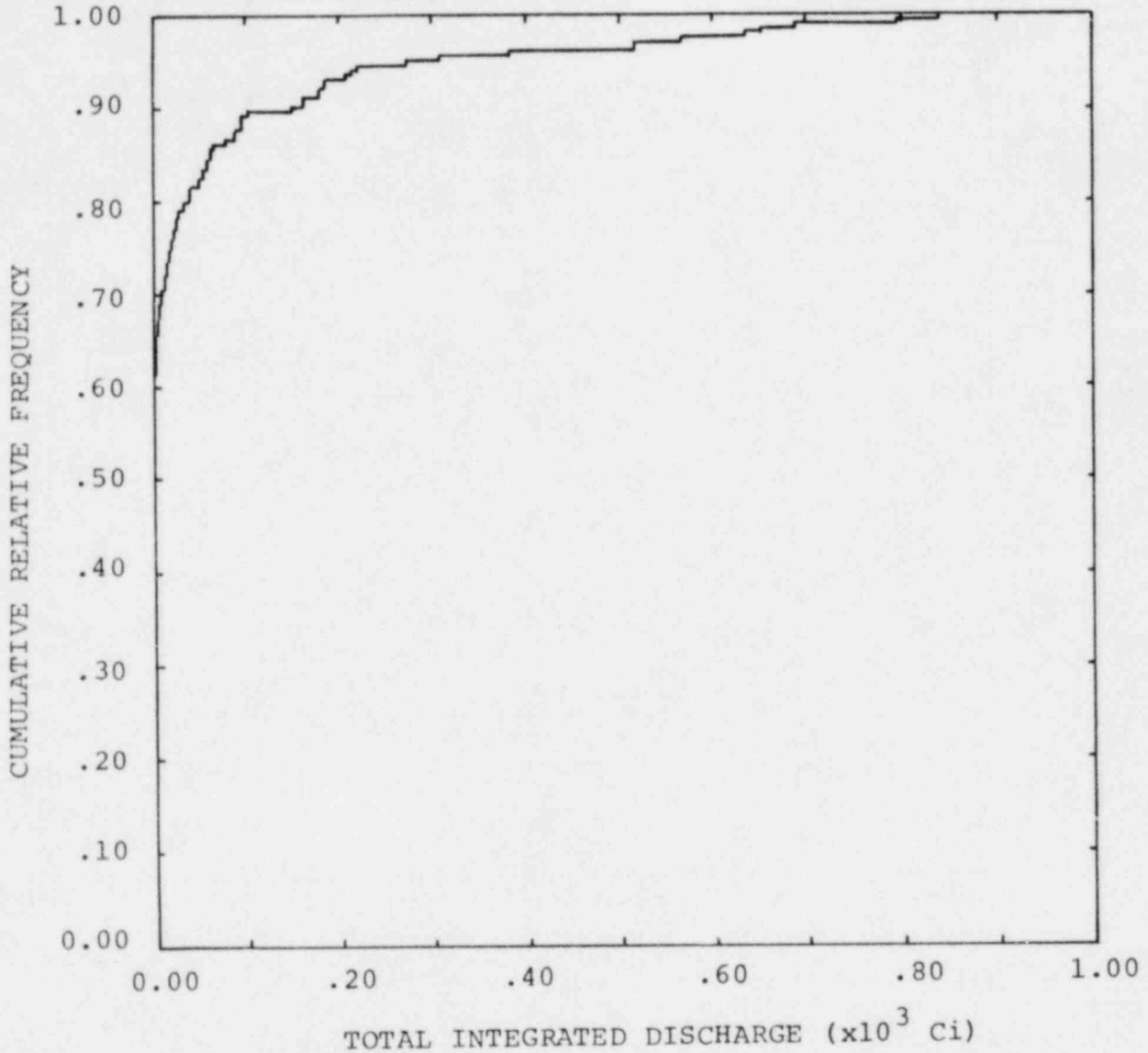

Figure 20. Cumulative Relative Frequency Distribution for Total Discharge at River L from the U-Tube Scenario with Solubility-Limited Source. Radionuclide Half-Life is 10^4 Years.

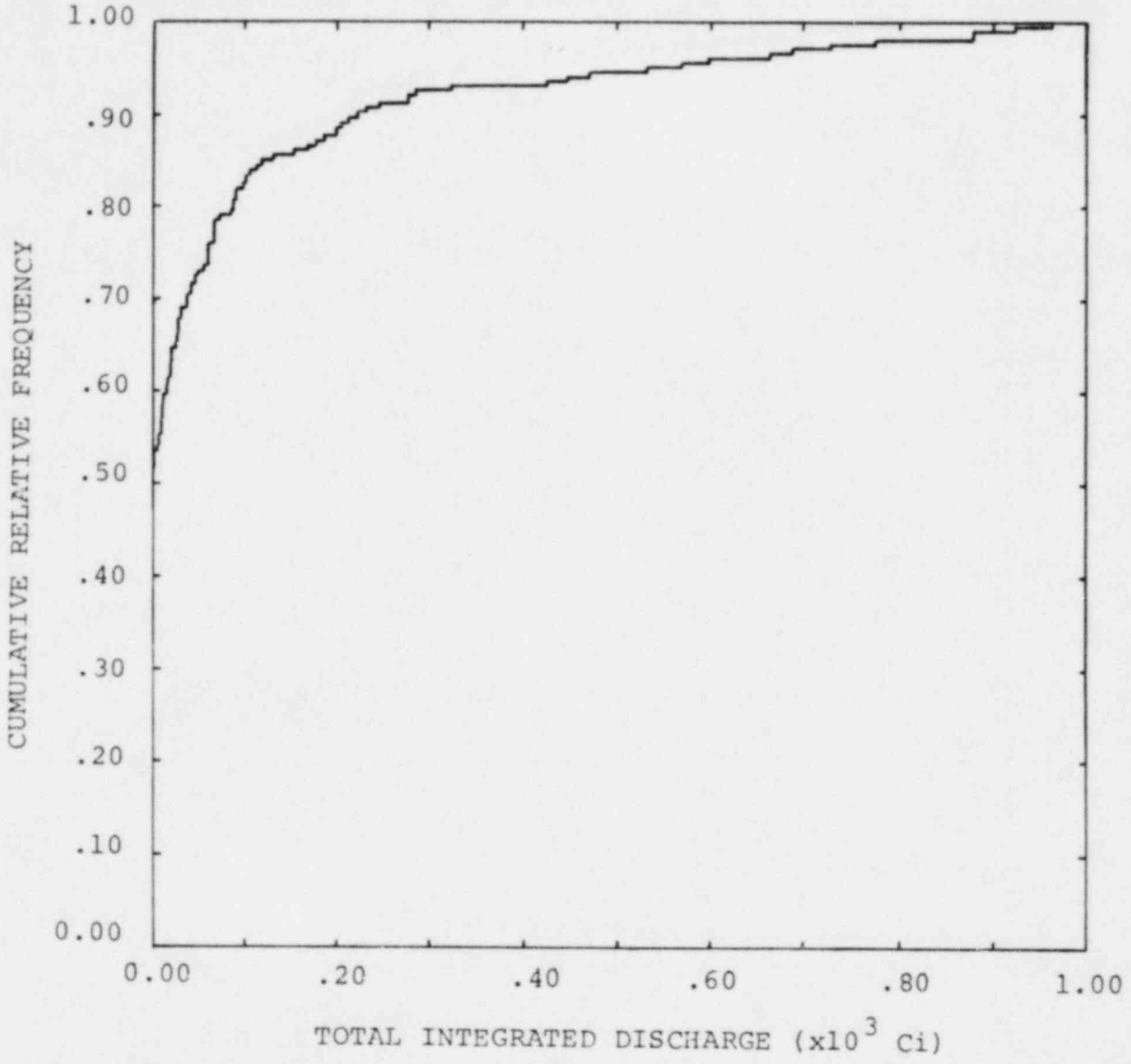

Figure 21. Cumulative Relative Frequency Distribution for Total Discharge at River L from the U-Tube Scenario with Solubility-Limited Source. Radionuclide Half-Life is 10^5 Years.

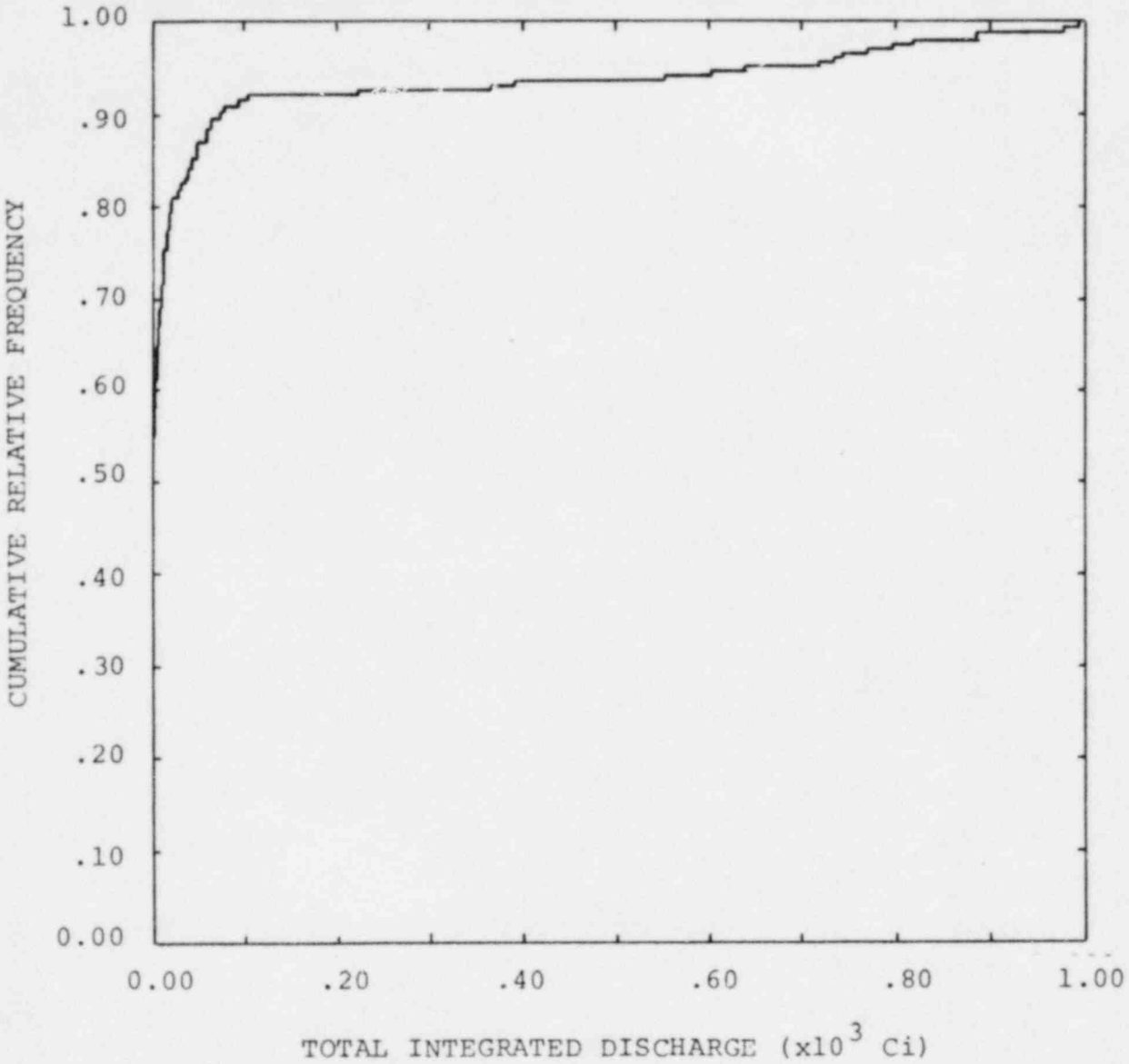

Figure 22. Cumulative Relative Frequency Distribution for Total Discharge at River L from the U-Tube Scenario with Solubility-Limited Source. Radionuclide Half-Life is 10^6 Years.

Table 9. Important Variables Selected by Stepwise Regression on Ranks for the U-Tube Scenarios with Solubility-Limited Source. Zero discharge included.

Half Life (years)	Variable Selected	Standardized Regression Coefficient	R^2
10^3	$(1/k_d)^2$	1.24	0.58
	$1/k_d$	-0.45	
	K_a/R_a	0.11	
	$K_s/(\phi_s R_s)$	0.09	
	$K_a C_s$	0.07	
10^4	$1/k_d$	0.48	0.57
	$(1/k_d)^2$	0.33	
	$K_s/(\phi_s R_s)$	0.18	
	$K_a C$	0.15	
10^4	$1/k_d$	1.20	0.63
	$(1/k_d)^2$	-0.36	
	$K_s C/\phi_s$	0.22	
	$K_a C_s$	0.16	
10^6	$1/k_d$	1.23	0.54
	$(1/R_s)^2$	0.62	
	C	0.27	
	K_s/R_s	0.19	
	$C K_s$	0.12	

as important. When zero discharge results are excluded (Table 10), the quality of the response-surface fits improves.

Rank correlation coefficients as a function of half-life for $1/k_d$ and C are shown in Figure 23. As in the leach-limited case, $1/k_d$ is used as it is the dominant variable controlling migration time. The solubility limit, C, is the dominant variable controlling the source rate. Once again, the importance of migration time decreases while the importance of source rate increases with increasing half-life.

5.3 U-Tube Scenario with Well Discharge

This scenario is identical to the previous scenario except that radionuclide discharge occurs at a nearby well (see Figure 6). Thus the radionuclide migration path is considerably shorter for this scenario than for the previous one. Well discharge is simulated by simply withdrawing a fraction (in this case, 1%) of the contaminated fluid. Because of the similarity in results for the leach and solubility-limited cases, only the solubility limited source is considered for this scenario.

Cumulative distributions for total discharge are shown in Figures 24 through 27. The results are similar in form to those obtained for the previous scenario with a solubility limited source. However, the maximum discharge is 10 curies more because only 1 percent of the contaminated water is allowed to discharge via wells.

Important variables, selected by stepwise regression on ranks, are shown in Table 11. The important variables selected

Table 10. Important Variables Selected by Stepwise Regression on Ranks for the U-Tube Scenario with Solubility-Limited Source. Zero Discharge Excluded.

Half Life (years)	Variables Selected	Standardized Regression Coefficient	R^2	N
10^3	$1/R_s$	1.23	0.83	83
	$(1/R_s)^2$	-0.71		
	$C\ K_s$	0.39		
	$K_a/(\phi_a R_a)$	0.34		
10^4	$1/k_d$	1.85	0.89	111
	$(1/k_d)^2$	-1.28		
	$K_a\ C$	0.33		
	$K_s/(\phi_s R_s)$	0.24		
	$K_s\ C$	0.18		
10^5	$1/k_d$	1.60	0.86	125
	$(1/k_d)^2$	-1.33		
	$K_s/(\phi_s R_s)$	0.42		
	C	0.38		
	$C\ K_a/\phi_a$	0.31		
10^6	K_s/k_d	1.17	0.82	126
	K_s/R_s	-0.68		
	C	0.62		
	$C\ K_a/\phi_a$	0.21		

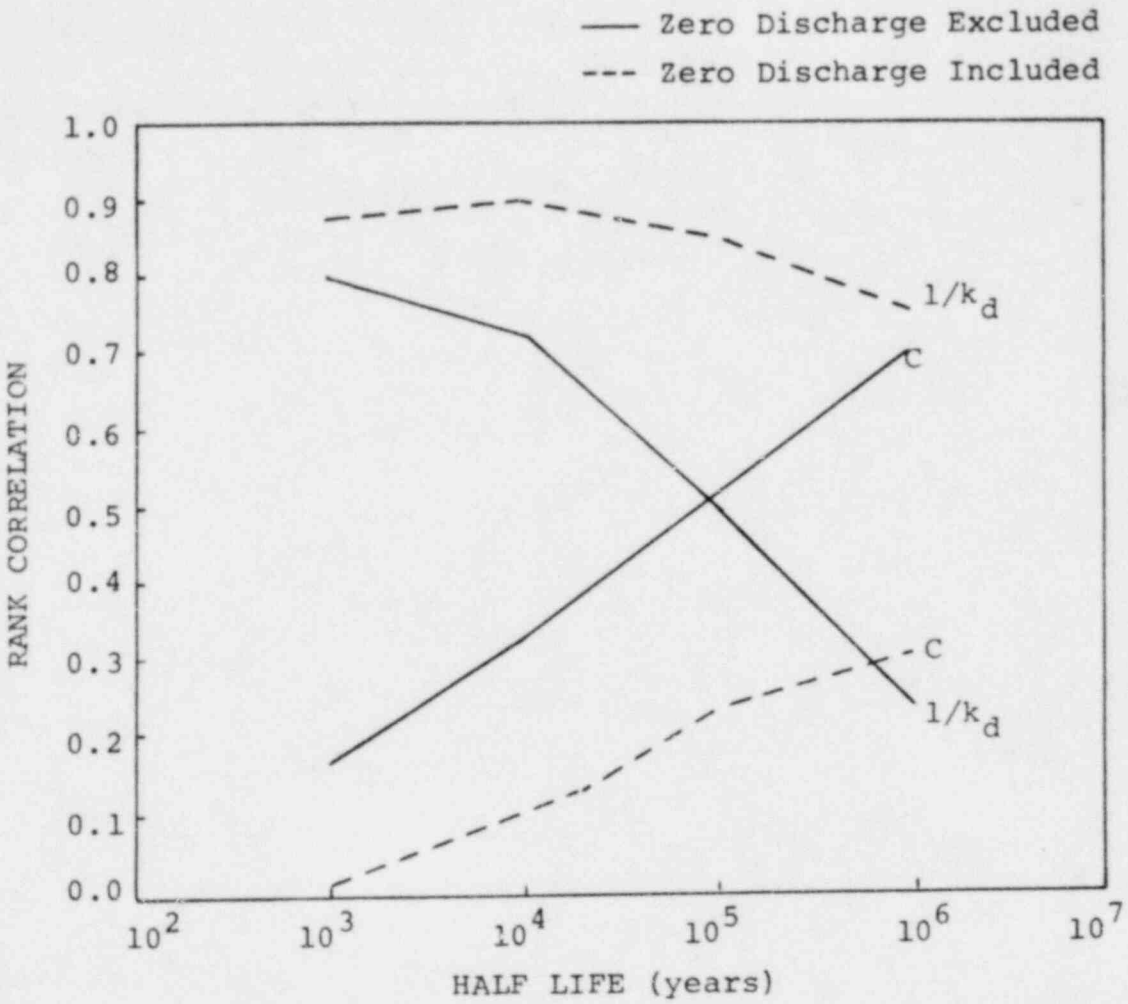

Figure 23. Rank Correlation Coefficients as a Function of Half Life for $1/k_d$ and C. U-tube Scenario with Solubility-Limited Source.

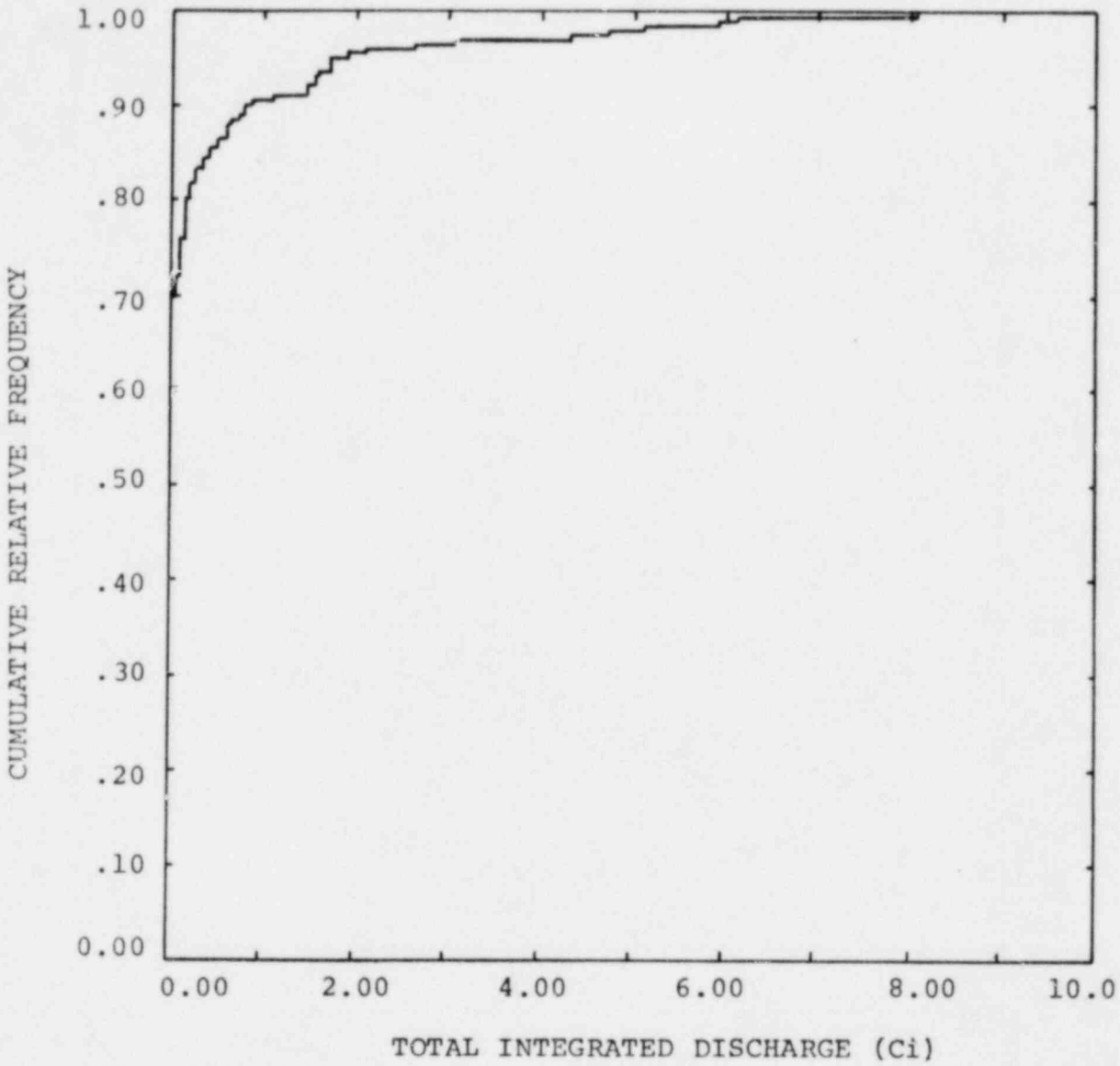

Figure 24. Cumulative Relative Frequency Distribution for Total Discharge at a Nearby Well from the U-Tube Scenario with Solubility-Limited Source. Radionuclide Half-Life is 10^3 Years.

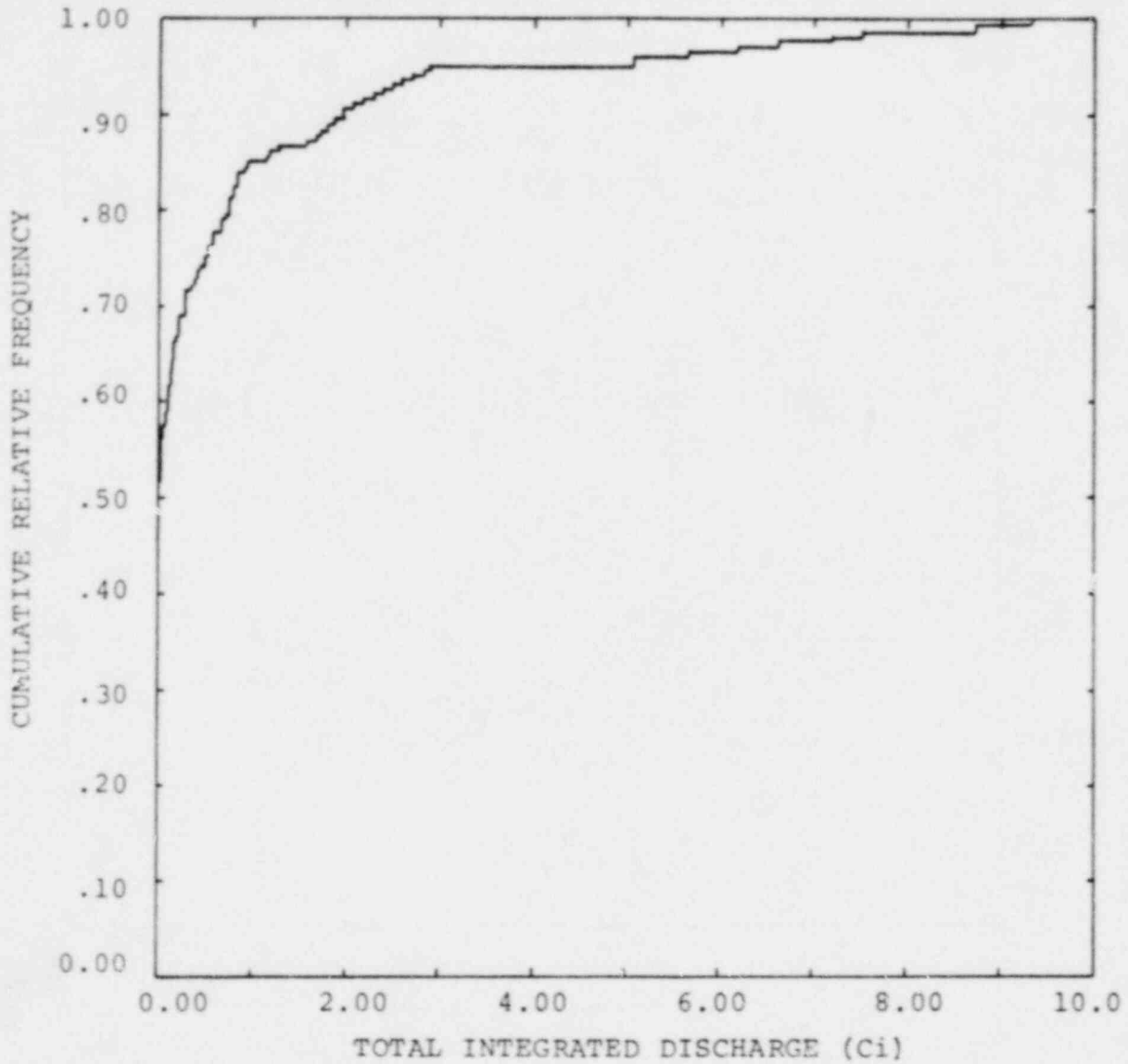

Figure 25. Cumulative Relative Frequency Distribution for Total Discharge at a Nearby Well from the U-Tube Scenario with Solubility-Limited Source. Radionuclide Half-Life is 10^4 Years.

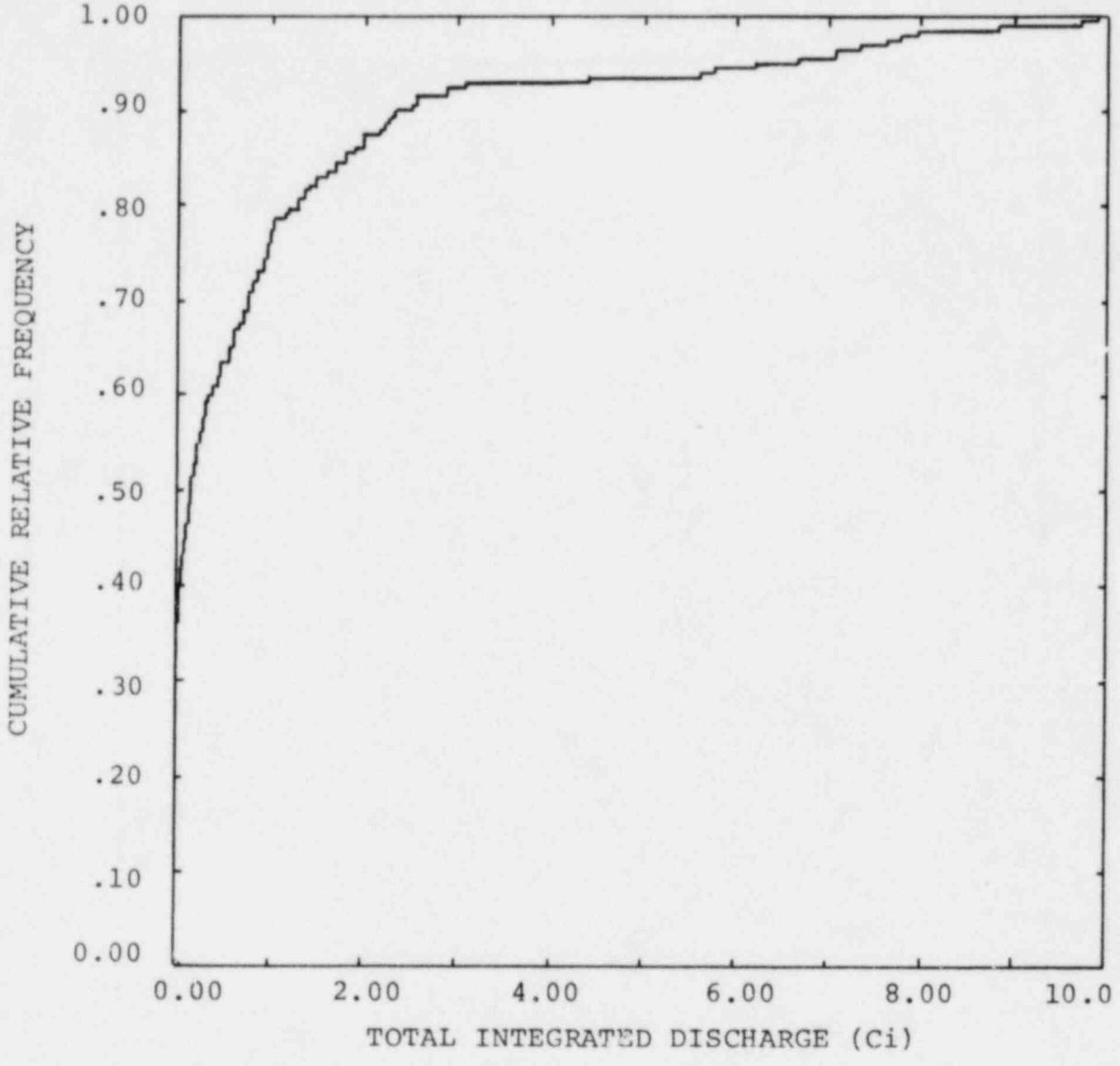

Figure 26. Cumulative Relative Frequency Distribution for Total Discharge at a Nearby Well from the U-Tube Scenario with Solubility-Limited Source. Radionuclide Half-Life is 10^5 Years.

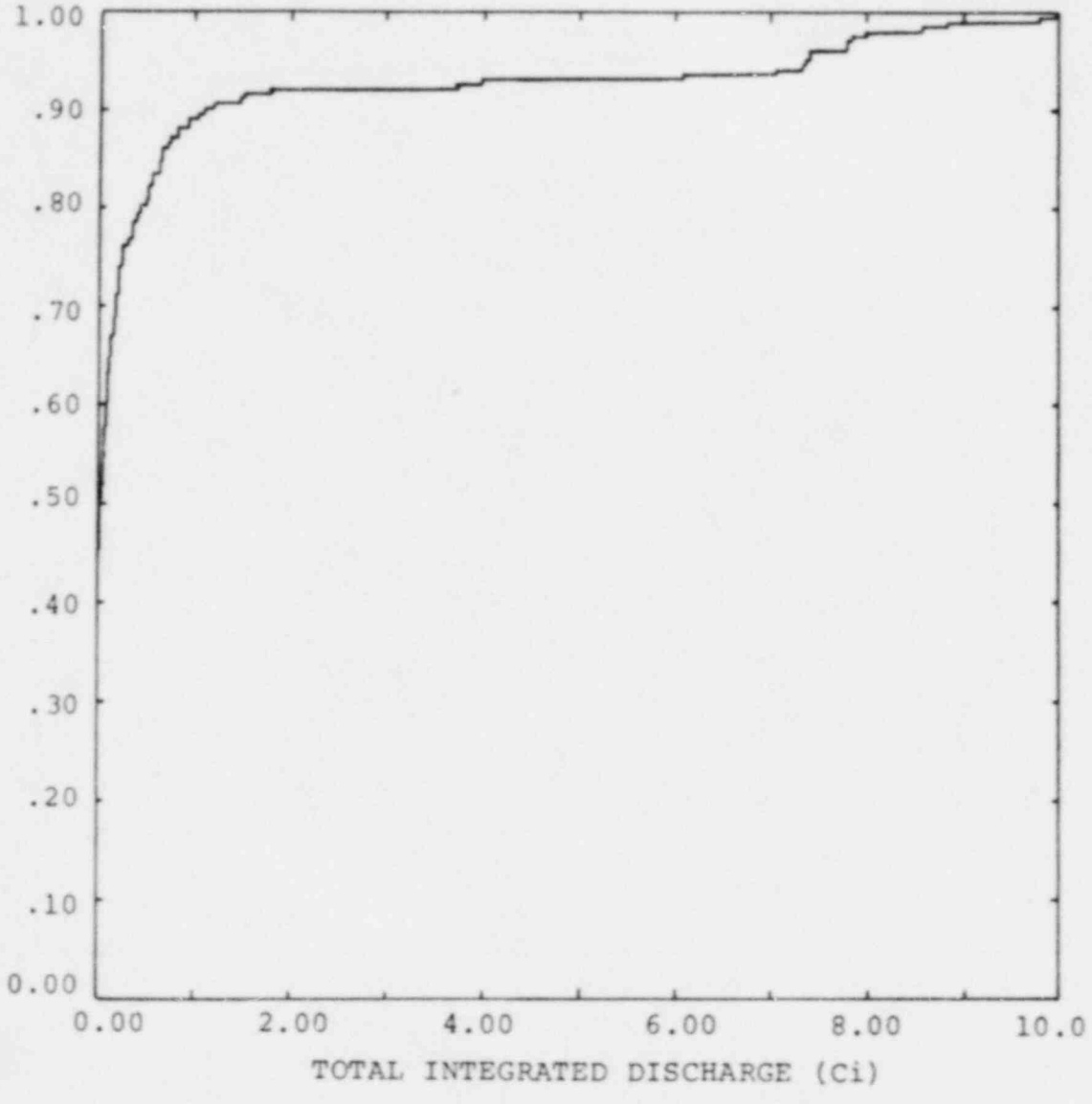

Figure 27. Cumulative Relative Frequency Distribution for Total Discharge at a Nearby Well from a U-Tube Scenario with Solubility-Limited Source. Radionuclide Half-Life is 10^6 Years.

Table 11. Important Variables Selected by Stepwise Regression on Ranks for U-Tube Scenario with Well Discharge and Solubility-Limited Source. Zero Discharge Excluded.

Half Life (years)	Variables Selected	Standardized Regression Coefficient	R^2	N
10^3	$1/k_d$	1.63	0.861	105
	$(1/k_d)^2$	-1.06		
	$K_s/(R_s\phi_s)$	0.37		
	C K_a	0.16		
10^4	$1/k_d$	2.25	0.836	137
	$(1/k_d)^2$	-1.32		
	C K_a	0.47		
	K_a/k_d	-0.26		
	C K_s/ϕ_s	0.22		
10^5	$1/k_d$	1.61	0.889	151
	$(1/R_a)^2$	-1.14		
	C K_s	0.43		
	C	0.34		
10^6	$1/k_d$	1.22	0.846	154
	$(1/k_d)^2$	-1.18		
	C	0.37		
	K_s/k_d	0.40		
	C K_s	0.18		

for this scenario should be compared with variables selected for the U-tube scenario with a solubility limited source and radionuclide discharge at River L (Table 10). There are only minor differences in the lists of important variables. The distribution coefficients (whether it appears as k_d, R_a, or R_s) still dominates variation of the migration time and thus remains the most important variable. The solubility limit dominates variation of the source rate and becomes more important as half life increases. This latter effect is shown more clearly in Figure 28 where the rank correlation coefficients for $1/k_d$ and C with total discharge are shown as a function of half life. The results shown in Figure 28 are, for practical purposes, virtually identical to the corresponding results for the previous scenario (Figure 23).

5.4 Hydraulic Connection Between Overlying and Underlying Aquifers

In this third scenario radionuclides migrate from the depository to the underlying aquifer then to River L (see Figures 8 and 9). The total migration time to River L is longer for this scenario than for the U-tube scenario because the interstital fluid velocity is lower for the underlying aquifer than for the overlying aquifer. The migration path length is also slightly longer for this scenario than for the U-tube with discharge to River L but the difference is insignificant.

Cumulative frequency distributions for total discharge are shown in Figure 29 through 32. The effect of the increased migration time can be seen by comparing Figures 29 through 32 with

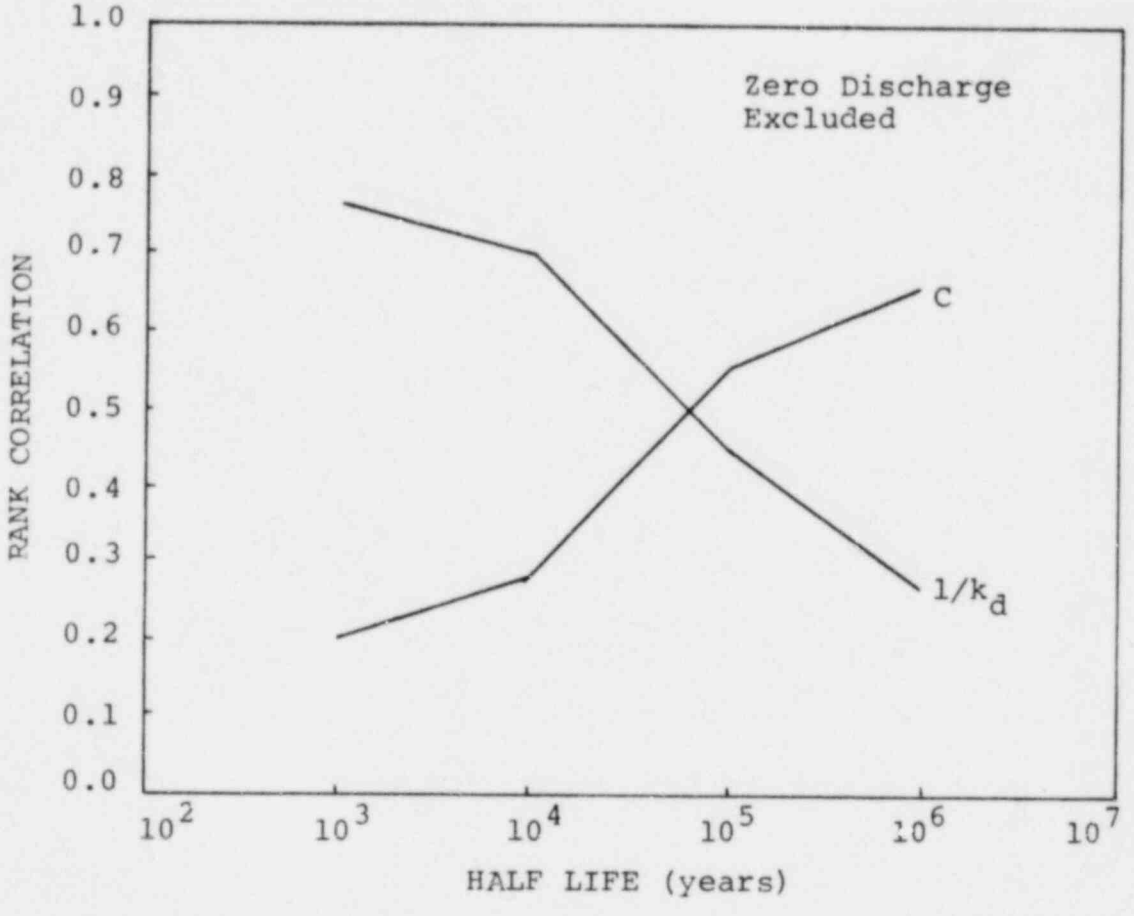

Figure 28. Rank Correlation Coefficients as a Function of Half-Life for $1/k_d$ and C. U-Tube Scenario with Well Discharge with Solubility-Limited Source.

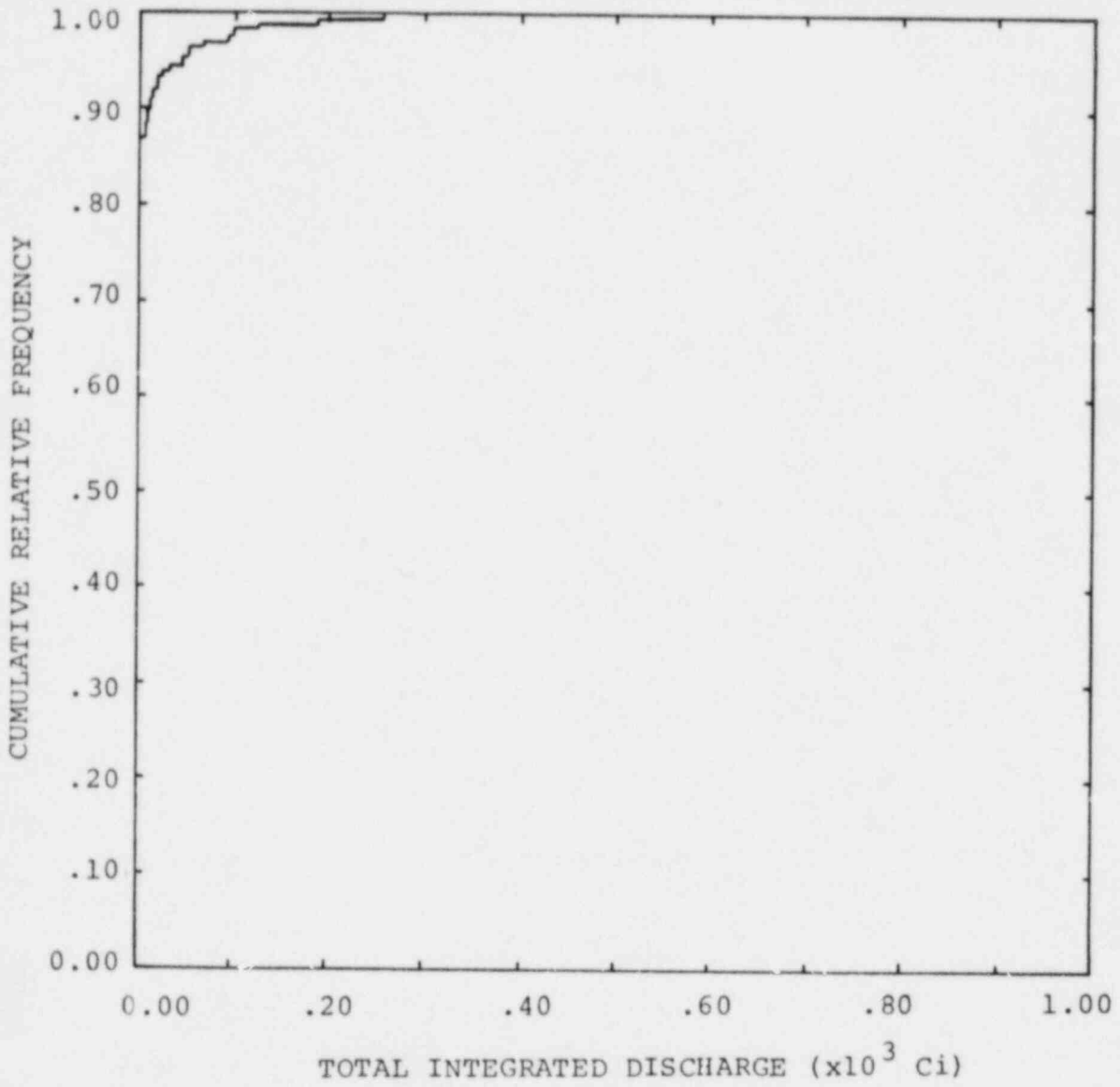

Figure 29. Cumulative Relative Frequency Distribution for Total Discharge at River L from Scenario 3 with a Solubility-Limited Source. Radionuclide Half-Life is 10^3 Years.

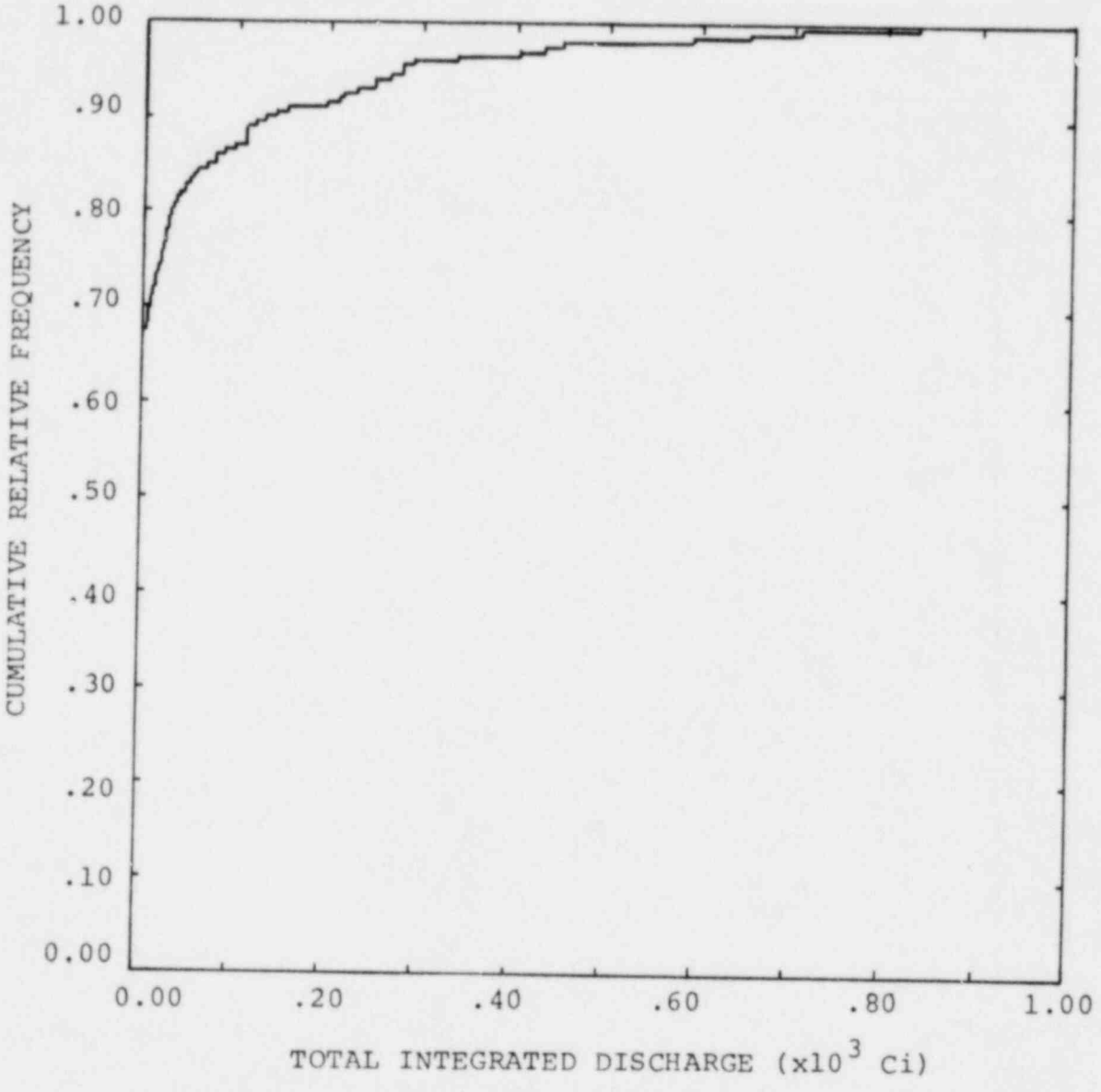

Figure 30. Cumulative Relative Frequency Distribution for Total Discharge at River L from Scenario 3 with a Solubility-Limited Source. Radionuclide Half-Life is 10^4 Years.

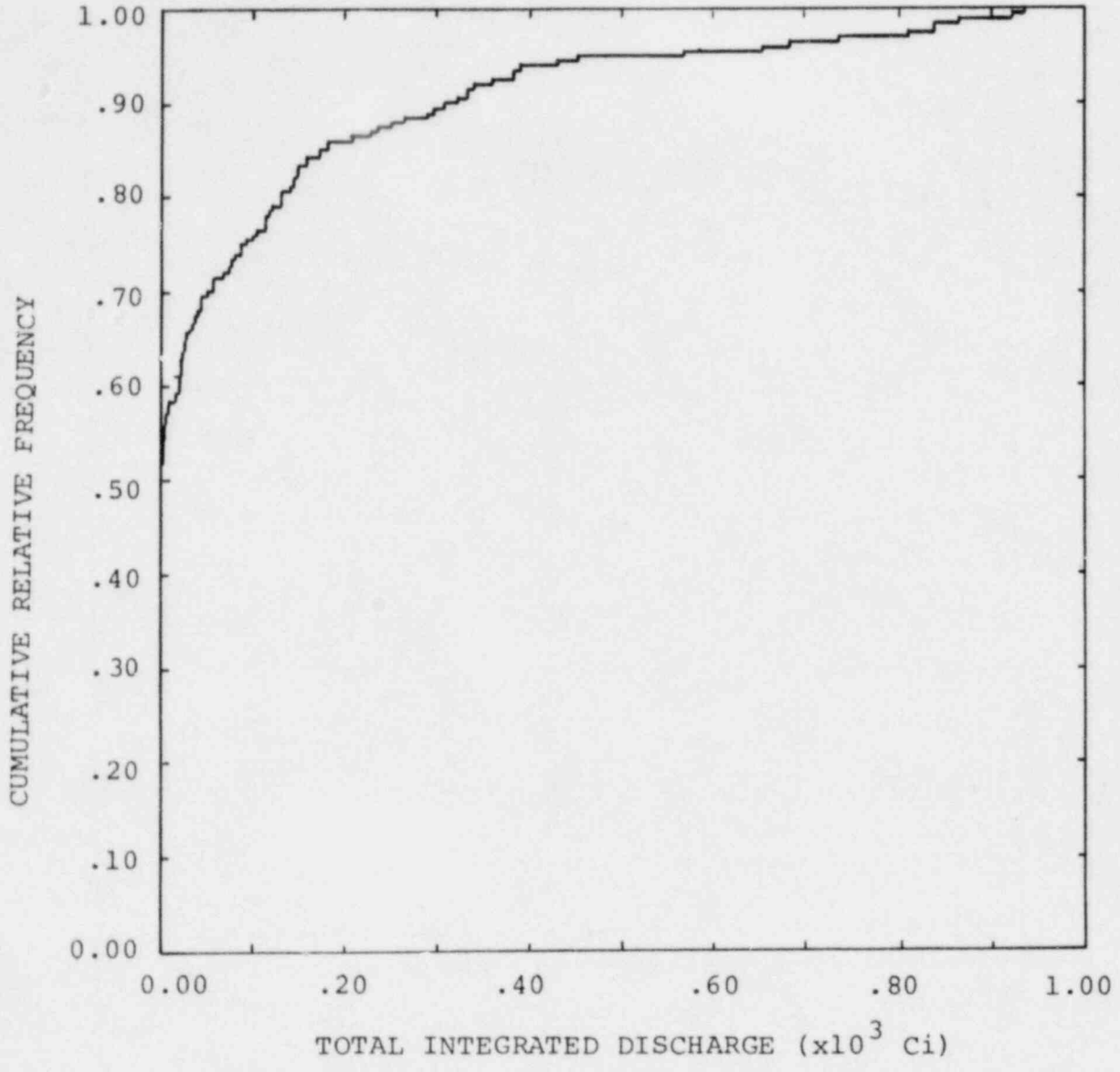

Figure 31. Cumulative Relative Frequency Distribution for Total Discharge at River L from Scenario 3 with a Solubility-Limited Source. Radionuclide Half-Life is 10^5 Years.

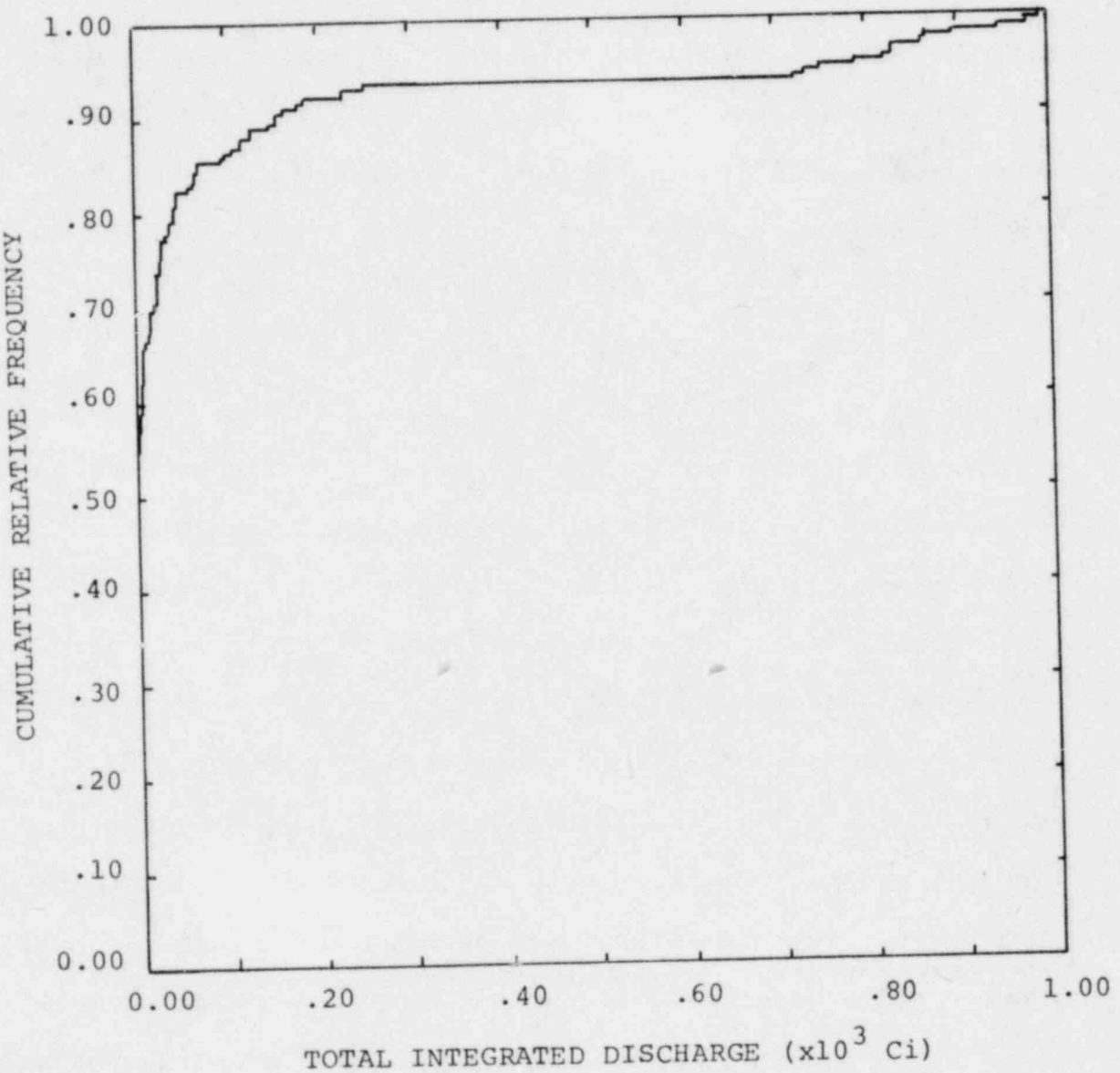

Figure 32. Cumulative Relative Frequency Distribution for Total Discharge at River L from Scenario 3 with a Solubility-Limited Source. Radionuclide Half-Life is 10^6 Years.

Figures 19 through 22. As should be expected, the increased migration time decreases total discharge. Important variables, as selected by stepwise regression on ranks, are shown in Table 12. Rank correlation coefficients with total discharge are shown for C and $1/k_d$ as a function of half life in Figure 33. For both the correlation coefficients and important variable selection, there is no practical difference between this scenario and the two previously considered scenarios.

VI. RESULTS AND CONCLUSIONS

In the previous chapters, a sensitivity analysis methodology has been presented and sensitivity analysis results have been shown. There are three principal elements underlying the investigation. First there is the reference site itself. This site, though hypothetical, has geologic and hydrologic properties which are characteristic of real sites. The response variable of interest is radionuclide discharge to the biosphere. Second, there are the groundwater transport simulators used to determine such discharges. Two models are considered, namely SWIFT and NWFT. The former is a very general multi-dimensional, numerical model. The latter is an analytic network flow model with a one-dimensional radionuclide transport capability. The objective in using both models is to demonstrate the applicability of the simplified model for statistical analyses. Finally, there are the statistical techniques for sensitivity analysis. These techniques have been

Table 12. Important Variables Selected by Stepwise Regression on Ranks for Hydraulic Connection through Depository and Solubility Limited Source. Zero Discharge Excluded.

Half Life (years	Variables Selected	Standardized Regression Coefficient	R^2	N
10^3	$1/R_a$	1.45	0.856	69
	$(1/R_a)^2$	-.92		
	C K_a	.36		
	$K_a/(\phi_a R_a)$	.30		
	$K_s/(R_s\phi_s)$	.20		
10^4	$1/k_d$	1.57	0.864	101
	$(1/k_d)^2$	-.98		
	$K_s/(R_s\phi_s)$	.35		
	C K_a	.34		
	C	.13		
10^5	$1/k_d$	1.77	0.884	111
	$(1/k_d)^2$	-1.21		
	C K_s	.41		
	C	.38		
10^6	$1/R_s$	.87	.0783	111
	$(1/R_a)^2$	-.74		
	C	.58		
	K_s/k_d	.33		
	$1/\phi_s$	.29		
	C K_s	.26		

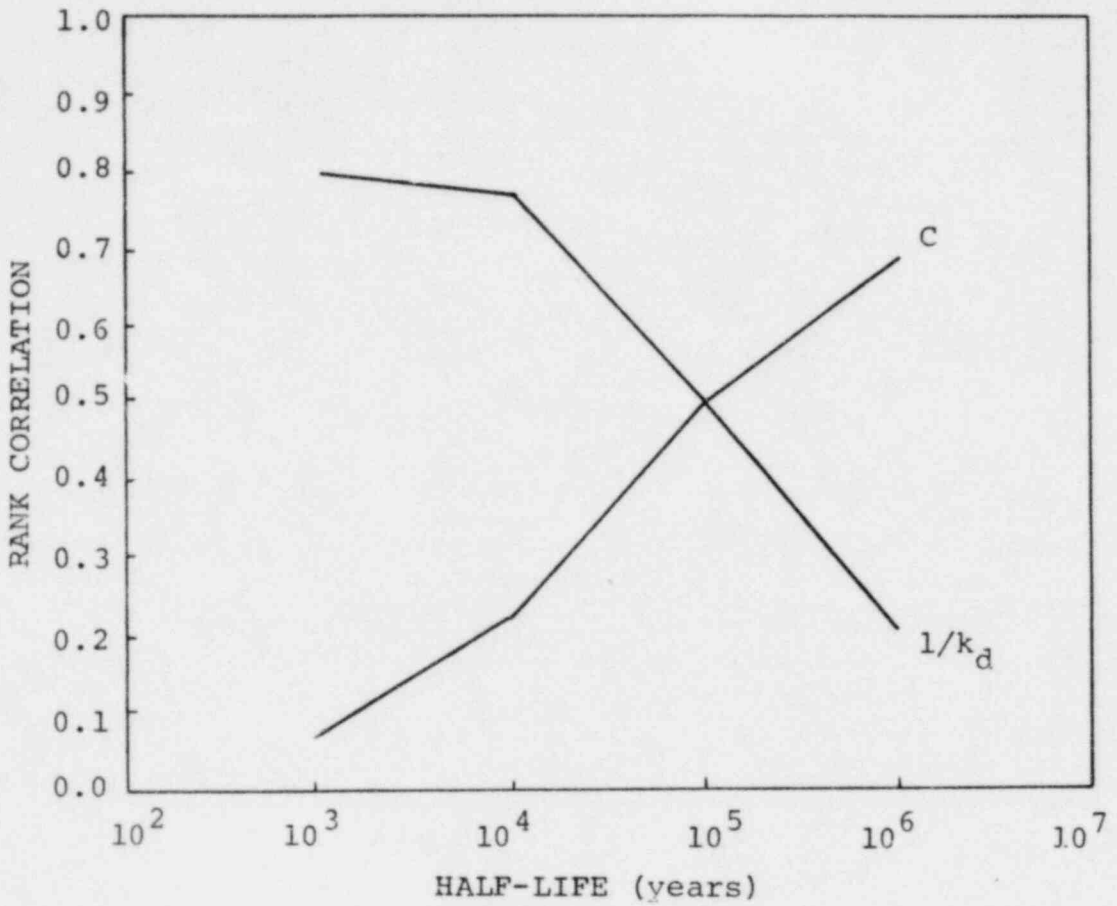

Figure 33. Rank Correlation Coefficients as a Function of Half-Life for $1/k_d$ and C. Connection to Lower Aquifer with Solubility-Limited Source.

designed to minimize the number of calculations required to examine the sensitivity of model output to model input.

Within the above mentioned framework, numerous calculations have been performed and several conclusions have been drawn. The first conclusion is that a simplified transport model, such as NWFT, may be quite adequate for repetitive calculations required in sensitivity and risk analysis. There are, of course, complicated problems involving heat, brine transport or geometrical complexities which are not amenable to such a simplified treatment. Thus a comprehensive risk methodology requires both a simple, efficient transport capability such as represented by NWFT, and a more general model such as SWIFT.

The second conclusion is that sensitivity analyses may be performed on a few selected scenarios to single out important variables.

In the present study, two variables were generally found to be important for each scenario. For solubility-limited cases, the important variables were the solubility limit and the distribution coefficient. For leach-limited cases, the most important variables were leach time and, again, distribution coefficient. Thus for each scenario, a migration-time variable and a source-rate variable were generally selected as most important. For different variable ranges and distributions, it would be possible for the sensitivity analysis to select variables other than the ones indicated above. However, the point here is that given variable ranges and distributions, variable importance is only weakly influenced by the scenario itself.

The third conclusion of this analysis simply adds some perspective and support to the second conclusion stated above. The conclusion is that the relative importance of variables which control radionuclide migration time (e.g., distribution coefficient and permeability) decreases as radionuclide half life increases whereas the relative importance of variables which control source rate (e.g., solubility limit or leach time) increases as radionuclide half life increases.

BIBLIOGRAPHY

Burkholder, H. C. and Rosinger, E. L. J. (1980), A Model for the Transport of Radionuclides and Their Decay Products through Geological Media, ONWI-11, Office of Nuclear Waste Isolation, Battelle Memorial Institute, Columbus, OH.

Campbell, J. E., Dillon, R. T., Tierney, M. S., Davis, H. T., McGrath, P. E., Pearson, F. J., Shaw, H. R., Helton, J. C., and Donath, F. A., (1978), Risk Methodology for Geologic Disposal of Radioactive Waste: Interim Report, SAND78-0029, Sandia National Laboratories, Albuquerque, NM.

Campbell, J. E., Kaestner, P. C., Langkopf, B. S., and Lantz, R. B. (1980), Risk Methodology for Geologic Disposal of Radioactive Waste: The Network Flow and Transport (NWFT) Model, SAND79-1920, Sandia National Laboratories, Albuquerque, NM.

Dillon, R. T., Lantz, R. B., and Pahwa, S. B. (1978), Risk Methodology for Geologic Disposal of Radioactive Waste: The Sandia Waste Isolation Flow and Transport (SWIFT) Model, SAND78-1267, Sandia National Laboratories, Albuquerque, NM.

Franke, O. L. and Cohen, P. (1972), Regional Rates of Groundwater Movement on Long Island, New York, U.S. Geological Survey, Prof. Paper 800-C.

Helton, J. C. and Iman, R. L. (1980), Risk Methodology for Geologic Disposal of Radioactive Waste: Sensitivity Analysis of the Pathways Model, SAND79-1393, Sandia National Laboratories, Albuquerque, NM.

Iman, R. L. and Conover, W. J. (1979), "The Use of the Rank Transformation in Regression," Technometrics, 21, pp. 499-509.

Iman, R. L., Helton, J. C., and Campbell, J. E. (1978), Risk Methodology for Geologic Disposal of Radioactive Waste: Sensitivity Analysis Techniques, SAND78-0912, Sandia National Laboratories, Albuquerque, NM.

McKay, M. D., Conover, W. J., and Beckman, R. J. (1979), "A Comparison of Three Methods for Selecting Values of Input Variables in the Analysis of Output from a Computer Code," Technometrics, 21, pp. 239-245.

DISTRIBUTION:

US Nuclear Regulatory Commission
NRC Standard Distribution GF (375 cys)
Division of Document Control
Distribution Services Branch
7920 Norfolk Avenue
Bethesda, MD 20014

Probabilistic Analysis Staff (36)
Office of Nuclear Regulatory Research
US Nuclear Regulatory Commission
Washington, DC 20555
Attn: M. C. Cullingford (35)
F. Rowsome

Division of Safeguards, Fuel Cycle and
Environmental Research (2)
Office of Nuclear Regulatory Research
US Nuclear Regulatory Commission
MS 1130SS
Washington, DC 20555
Attn: F. Arsenault
C. Jupiter

Division of Waste Management (4)
Office of Nuclear Material Safety and
Safeguards
US Nuclear Regulatory Commission
Washington, DC 20555
Attn: J. Malaro
M. Bell
J. Martin
L. Rossbach

US Geologic Survey (2)
US Department of Interior
Denver Federal Center
Denver, CO 80225
Attn: D. B. Grove
L. F. Konikow

The Analytical Sciences Corporation
Six Jacob Way
Reading, MA 01867
Attn: J. W. Bartlett
C. Koplik

INTERA Environmental Consultants, Inc. (15)
11999 Katy Freeway
Houston, TX 77079
Attn: R. Lantz (4)
M. Reeves (10)
D. Ward

Lawrence Livermore Laboratory (2)
P. O. Box 808
Livermore, CA 94550
Attn: A. Kaufman, L-156
D. Isherwood, L-224

David Hodgkinson
Theoretical Physics Division
Building 8.9
AERE Harwell
Oxfordshire OX11/RA
England

A. J. Soinski
California Energy Commission
Nuclear Assessments Office
1111 Howe Avenue, MS #35
Sacramento, CA 95820

Science Applications, Inc.
1200 Prospect Street
P. O. Box 2351
La Jolla, CA 92037
Attn: E. Straker

Pierre Pages
Boite Postale No. 48
92260 Fontenay-Aux Roses
France

D. R. Proske
Duetsche Gesellschaft fur Wiederaufarbeitung
von Kernbrennstoffen mbH
Bunteweg 2, 3000 Hannover 71
West Germany

Cathy Fore
Ecological Sciences Information Center
Oak Ridge National Laboratory
P. O. Box X
Oak Ridge, TN 37830

Stephan Ormonde
Quantum Systems, Inc.
P. O. Box 8575
Albuquerque, NM 87198

Lyn Gelhar
Department of Geoscience
New Mexico Tech
Socorro, NM 87801

John Buckner
E. I. DuPont
Savannah River Laboratory
Aiken, SC 29801

Hans Haggblom
Studsvik Energi Teknik AB
S-611 82 Nykoping
Sweden

Donald E. Wood
Rockwell Hanford Operations
202-S Building
200 West Area
P. O. Box 800
Richland, WA 99352

Larry Rickartsen
Science Applications, Inc.
P. O. Box 843
Oak Ridge, TN 37830

Dan H. Holland, President
New Millennium Associates
1129 State Street, Suite 32
Santa Barbara, CA 93101

V. K. Barwell
Environmental Research Branch
Atomic Energy of Canada Limited
Research Company
Chalk River, Onatario
Canada KOJ1JO

Paul Kruger
Department of Civil Engineering
Stanford University
Stanford, CA 94305

Ken Dormuth
Environmental and Safety Branch
Atomic Energy of Canada, LTD
Whiteshell Nuclear Research
Establishment
Pinawa, Manitoba
Canada ROE1LO

Mark Goldstein
JGC Corporation
14-1, Bessho 1-Chome
Minami-Ku
Yokohama, 232 Japan

400 C. Winter
1223 R. L. Iman (25)
1223 R. G. Easterling
4000 A. Narath
4231 S. A. Dupree
4400 A. W. Snyder
4410 D. J. McCloskey
Attn: J. W. Hickman
G. B. Varnado
L. D. Chapman
4413 N. R. Ortiz
4413 D. C. Aldrich
4413 J. E. Campbell (25)
4413 M. Chu
4413 R. M. Cranwell
4413 F. A. Donath
4413 N. C. Finley
4413 J. C. Helton
4413 D. E. Longsine
4413 S. J. Niemczyk
4413 L. T. Ritchie
4443 D. A. Dahlgren
4510 W. D. Weart
4511 G. E. Barr
4511 L. R. Hill
4514 M. L. Merritt
4515 M. S. Tierney
4530 R. W. Lynch
4536 D. M. Talbert
4737 P. C. Kaestner
3141 T. L. Werner (5)
3151 W. L. Garner (3)
8266 E. A. Aas
3154-3 R. P. Campbell (25)
for NRC distribution
to NTIS